63-3-4

UNCLASSIFIED

RTD-TDR-63-9, Vol I

FINAL TECHNICAL REPORT
EVALUATION AND MODIFICATION OF
EXISTING PROTOTYPE DYNAMIC CALIBRATION
SYSTEM FOR PRESSURE-MEASURING TRANSDUCERS
VOLUME I TECHNICAL RESULTS

TECHNICAL DOCUMENTARY REPORT NO RTD-TDR-63-9, VOL I
March 1963

6593d Test Group (Development)
Air Force Flight Test Center
Edwards Air Force Base, California

Project No 3850 BPSN 3850, Task No 38506

(Prepared under Contract No AF 04(611) 8199
by Houston Engineering Research Corporation
Houston, Texas)

UNCLASSIFIED

RTD-TDR-63-9, Vol I

FINAL TECHNICAL REPORT
EVALUATION AND MODIFICATION OF
EXISTING PROTOTYPE DYNAMIC CALIBRATION
SYSTEM FOR PRESSURE-MEASURING TRANSDUCERS
VOLUME I TECHNICAL RESULTS

TECHNICAL DOCUMENTARY REPORT NO RTD-TDR-63-9, VOL I
March 1963

6593d Test Group (Development)
Air Force Flight Test Center
Edwards Air Force Base, California

Project No 3850 BPSN 3850, Task No 38506

(Prepared under Contract No AF 04(611) 8199
by Houston Engineering Research Corporation
Houston, Texas)

FOREWORD

This is the Final Technical Report under Air Force Contract AF 04(611) 8199 (HERCO Project 106), Evaluation and Modification of Existing Prototype Dynamic Calibration System for Pressure-Measuring Transducers. The prototype system was built by Dresser Dynamics under Contract AF 04(611)4568.

Background for this project was acquired by HERCO through preparation of a monograph for the National Bureau of Standards on the subject "Methods for the Dynamic Calibration of Pressure Transducers". The work on this monograph was done under subcontract with SIE Division of Dresser Electronics. Contract numbers are NBS Contract S-14226-61 for the prime contract between SIE and NBS and DE 8130 for the subcontract between SIE and HERCO.

The current project was started under the management of Douglas Muster, and L C Eichberger did the initial work on the mathematical analysis. The authors of this report are

Joseph L Schweppe (Project Manager), Abstract and Evaluation of Pressure Transducer Calibration System

James L Williams, Shock-Tube System

Arthur H McMorris, Mathematical Analysis and Computer Programs

W Ray Busby, Data Recording System

The project has benefited greatly from the supervision and cooperation of William A Wright, Air Force Project Engineer.

This Abstract Is Unclassified

ABSTRACT

The work under this contract was undertaken with six specific goals: (1) to evaluate the pressure transducer calibration facility at Edwards Air Force Base, (2) to determine what minor and major modifications were required to provide a highly accurate calibration system with an output compatible with IBM data processing formats, (3) to make approved minor modifications and test the resulting system, (4) to find and justify rigorous mathematical methods for determining the dynamic characteristics of a pressure transducer based on information obtained from transient response measurements, (5) to find and justify rigorous mathematical methods for determining the input function to a transducer based on the output data and the dynamic characteristics, and (6) to develop computer programs to perform the computations for each mathematical method. Volume I of this report summarizes the results of the entire program and presents both conclusions and recommendations for future work. Volume II is an operating manual which covers the application of the results to calibration, evaluation and use of pressure transducers. And Volume III covers the computer programs.

After minor modifications the system can be used effectively for recording, digitizing and punching the experimental calibration data. It has been established that the transfer function can be computed accurately by numerical methods, and that, for short-time records, the input function can be computed given the response and the transfer function. The accuracy of the computation is limited by the accuracy with which the data can be determined with the data reduction system. While the computation using the inverse transfer function is successful, limitations imposed by data sampling requirements seriously limit the usefulness of the method. Since each output data point requires a substantial computation process, computer time requirements are prohibitive for all except very short time records.

Recommendations for further work include addition of a calibration waveform generator, an investigation of the analog inverse-transform computer, and an investigation of the effect of temperature on the characteristics of transducers.

TABLE OF CONTENTS

VOLUME I TECHNICAL RESULTS

VOLUME II OPERATING PROCEDURES

VOLUME III COMPUTER PROGRAMS

LIST OF SYMBOLS

SYMBOL	CONCEPT
a	local sonic velocity, $(\gamma RT)^{1/2}$
A	arbitrary constant function amplitude real part of Fourier transform
B	imaginary part of Fourier transform
C	arbitrary constant
e	base of Napierian or natural logarithm (e = 2.718...)
f	frequency input function
F	force Fourier transform of f Laplace transform of f maximum value of F
h	transfer function (time domain)
H	transfer function (frequency domain)
I	imaginary part of a complex number
j	square root of minus 1
m	mass
M	Mach number, v/a
n	n-th quantity or number in general
p	pressure
P	polynomial
Q	variable of polynomial, P
R	gas constant real part of a complex number
s	complex variable $\sigma + j\omega$
t	time
T	temperature upper limit of integration
U	shock velocity relative to rest
u	unit function particle velocity

SYMBOL	CONCEPT
v	velocity
x	function
X	Fourier transform of x real part of X (s)
Y	imaginary part of X (s)
γ	ratio of specific heats
Δ	finite difference
ϵ	arbitrary constant lower limit of integration
θ	angle, $\omega\Delta t$
ρ	mass density
σ	real part of $s = \sigma + j\omega$
τ	time interval, $N\Delta t$
ω	angular velocity
$\angle$	phase angle of function

SUPERSCRIPT

' (prime)	modified variable
i	index
k	index

SUBSCRIPT

k	k-th quantity or number in general
n	n-th quantity
N	point at which quantity becomes constant
r	reflected wave
o	impulse function
-1	step function
u	upper limit on time or frequency

SECTION I EVALUATION OF PRESSURE TRANSDUCER CALIBRATION SYSTEM

The objective of pressure transducer calibration is to determine the response of the transducer system to both static and dynamic inputs so, ultimately, dynamic input pressure-time relations can be determined from the transducer system response. A calibration facility must be evaluated by the degree to which this objective is met.

The calibration can be divided into three parts. (1) Static or pseudo-static calibration to determine transducer system output as a function of pressure input. (2) Dynamic calibration to determine the amplitude of the transducer system output as a function of pressure input. And (3) dynamic calibration to determine the system transfer function (both amplitude and phase characteristics). With the complete calibration available the pressure input may be computed, at least theoretically, for any given response.

The calibration furnishes the information to determine the rate or rates of change which will excite the transducer into resonance. For pressures which change at rates which are relatively slow compared to the rate of change associated with the lowest resonant frequency of the transducer, the pressure input can be obtained from the transducer response and the static calibration. For pressures which change at rates comparable to those associated with the resonant frequency of the transducer, the inverse transfer function must be used to compute the pressure input associated with a given response.

Ideally, transducers would be selected for each application so that operation would always be at rates of change far from those which would excite resonance. However, a given experimental problem may require transducer characteristics which cannot be obtained. In this case the only alternative is to use an available transducer with the best possible calibration. Even when the transducer is to be used for relatively low rates of pressure change, it is important to know the resonant frequencies.

This report covers the evaluation of the dynamic calibration facility at Edwards Air Force Base. It includes a description of the modifications to the facility made during the course of the work, recommended operating procedures, and recommendations for future work to further improve the facility. Static and pseudo-static calibration are not included per se.

SYSTEM AT BEGINNING OF WORK

The shock tube facility includes a 35 foot, 7/8-inch by 1 1/4-inch shock tube with the associated air supply and control system, Figure 1. The shock velocity is determined by measuring the time interval between the passage of the shock wave past two Atlantic Research Blast Velocity Gages placed 6-, 12-, or 24-inches apart along the length of the tube. The transducer system output is recorded by photographing the trace on a Tektronix RM 35 oscilloscope. The

photograph, on a Polaroid transparency, is read by a Dresser Dynamics Flying Spot Analog-to-Digital Converter. The output from the converter goes to a Hewlett-Packard Digital Recorder and a DYMEC Card Punch Coupler. The digitized output is printed on paper tape by the digital recorder. It is transmitted by the card punch coupler to an IBM 523 Summary Punch which punches the output on IBM cards.

Additional information is keypunched on other IBM cards which are added to the deck. This information includes the expansion chamber pressure, the time interval, the distance between the blast velocity gages, and the temperature of the shock tube. The transfer function for the transducer system is computed on an IBM 7090 computer, using a modified form of the program developed by Bowersox[1]* at Jet Propulsion Laboratory in 1957. At the beginning of this work there was no inverse transform program.

The system had a number of major shortcomings. (1) If the FSADC were stopped while the transparency was being scanned, it could not be started again without risk of error. The counter might jump either on stopping or starting. (2) The converter calibration drifts rapidly enough to make high speed analog-to-digital conversion desirable. The punch speed was less than the capability of the machine, so the time for drift was longer than necessary. (3) The IBM 523 Summary Punch was not synchronized with the analog-to-digital converter. (4) The output of the photomultiplier was not uniform as the scanning point moved across the film. (5) The program for computing the transfer function did not determine the correct phase relations. (6) The FSADC cannot distinguish between the trace and flaws in the transparency. No formal procedure for removing flaws had been developed. (7) There was no method for computing the pressure input to the transducer from the response and the transfer function. (8) Calibration data are not recorded on the transparency along with the transient response. And (9) there is no provision for calibration at other than ambient temperature.

The next subsection describes the effect of making several minor modifications. A detailed description of each modification is given in Section 4 of this report.

SYSTEM WITH MINOR MODIFICATIONS

Six of the shortcomings listed above were eliminated by minor modifications. The erratic operation of the FSADC counter was found to be caused by a loading change on the decade counter staircase outputs. The loading change resulted from transients induced on the -200 volt supply by the start and stop switches. Installation of current limiting resistors in the start and stop switch circuits solved the problem.

* Superscripts refer to Reference List.

The IBM 523 Summary Punch was synchronized with the analog-to-digital converter by adding a relatively simple diode gate circuit. The DYMEC Card Punch Coupler generates a signal for the purpose of holding the electronic counter during the punch cycle. This signal was utilized by adding a diode gate circuit to inhibit the advancing of the X-counter and the resetting of the Y-counter. The X16 scaler in the digital control unit was changed to X12 and the X4 scaler was changed to X3. The maximum summary punch rate of the IBM 523 is 50 cards per minute. The above changes make it possible to punch the output data at 40 cards per minute.

Variation of the output of the photomultiplier with scanning position because of misalignment of the tube was reduced by tube alignment, and by careful focusing of the cathode ray tube trace.

The computer program was modified to permit computation of both amplitude and phase characteristics of the transducer system. The modification of Bowersox's program was tested on one- and two-degree-of freedom analytic functions.

Procedures have been set up for using photographic retouching techniques on the transparencies. These procedures reduce the necessity for "filling in" data points which are recorded erroneously by the digitizer. For those points which are still in error, the operating procedures cover the details of editing.

A digital computer program was successfully developed for computing the input time function from the response and the transfer function. The usefulness of this program is limited by the data sampling requirements. In order to compute a time function over a period of one second, the transfer function must be computed at intervals of 0.5 cps. If computations are necessary to 10,000 cps, 20,000 data points are required. Over a hundred hours of IBM 7090 time would be required for these computations, so it is apparent that a more economical means is needed for solving the inverse transform problem.

After the minor modifications were made and the computer programs were written, the complete system was checked out. A series of transducer system responses were photographed, the responses were sampled, digitized and punched on IBM cards, the additional data required were key-punched, and the transducer system transfer function was computed. The results for four transducers are shown in Figures 2 through 5. Because of excessive machine time requirements, the input step was computed for only one of the transducers, Figure 6.

Figures 2 through 5 show that the transducers have complex characteristics, not accurately described by a simple one- or two-degree-of-freedom model. Figure 6 shows that the system transfer function can be used to obtain a reasonably accurate input time function. A more detailed discussion of the results is given in Section 3, Mathematical Analysis and Computer Programs.

SYSTEM WITH MAJOR MODIFICATIONS

Three of the shortcomings of the present system can be corrected only by making major modifications in the calibration procedures and/or facility. The first of these shortcomings is in the method for computing the input pressure from the transducer response and the transfer function. At the beginning of this project there was no method. Now the method which has been developed requires a prohibitive amount of computer time. It appears that an analog solution for the inverse transformation would be much more desirable than the digital solution. The analog technique holds promise of providing the output data in real time as it is produced. A preliminary investigation of the analog techniques indicates that stability and accuracy are opposing factors in systems which are based on active networks. Hence, the final answer probably will represent a compromise between active and passive networks. The solution will be determined only through a comprehensive and thorough investigation of the problem. The result should be a real time system which will convert the transducer output to an accurate pressure-time record.

The second of the shortcomings not corrected by minor modification is the lack of means for making the recording process independent of the calibration of the digitizing equipment. To accomplish this, calibration data must be included on the transparency along with the transient response of the transducer. The insertion of a calibrating waveform on the transparency should eliminate the need for frequent calibration of the data recording system and should improve the accuracy of the resulting digital output. This modification will require the design and construction of a precision waveform generator and changes in the present digital control system to permit digitizing the calibration data and the transient waveform simultaneously.

The third of the remaining shortcomings of the facility is that there is no provision for calibration at other than ambient temperatures. Since transducers are often used at elevated temperatures, a technique for calibration at elevated temperatures appears to be needed.

RECOMMENDATIONS FOR FURTHER WORK

Because the mathematical analysis has verified that accurate transfer functions can be obtained from truncated data, the present FSADC is satisfactory for obtaining and digitizing transient waveforms. The accuracy of the data determines the accuracy of the approximate transfer function, and the accuracy of the data is a strong function of system calibration. Insertion of a calibration waveform on each transient waveform transparency will increase the period between equipment calibrations, will simplify operational procedures, and will improve the accuracy of the digitized data. It is recommended that a calibration waveform generator be added to the Edwards AFB calibration facility.

Serious consideration should be given to the problem of developing a less cumbersome method of obtaining actual input time functions from a time

response and a known transfer function. An analog solution to this problem appears to be both possible and practical. It is recommended that a comprehensive investigation of the problem be undertaken with the following objectives: (1) determine a minimum configuration of active and passive elements required to compensate pressure transducers on a real time basis; (2) design and fabricate a prototype compensator system based on this minimum configuration; and (3) modify the digital computer program to determine the parameter settings for the compensator system from the computed transfer function.

Because transducers are used so frequently at elevated temperatures, consideration should be given to the problem of determining the effect of temperature on pressure transducer characteristics. It is recommended that a study be undertaken in five parts. (1) Make an analytical study to estimate the effect of temperature on peizoelectric, strain-gage, and capacitance type transducers. (2) Choose sample gages of each type and determine the transfer functions at various temperature levels. Use relatively simple equipment for these experiments since precise high-temperature calibrations are not needed at this stage. (3) Compare the predicted and actual temperature effects and evaluate the order-of-magnitude of the error resulting from the use of an ambient temperature calibration on data obtained at high temperature. (4) Report the level of uncertainty accepted when an ambient calibration is used for high temperature data, the relative effect of temperature on different types of transducers, and the need for improved cooling of transducers. And (5) make recommendations on the need for precise high temperature calibration facilities.

SECTION 2 SHOCK-TUBE SYSTEM

The shock-tube system consists of all equipment necessary to make a dynamic calibration, including the photographic record required to determine the amplitude and phase characteristics of the transducer. In the interest of simplicity and convenience, experimental work was performed on a prototype shock tube at the University of Houston rather than on the Edwards AFB Transducer Evaluation Shock Tube. Thus it was necessary to evaluate the suitability of the University of Houston shock tube as a prototype for the Edwards AFB tube, as well as to investigate the use of these shock tubes in a dynamic calibration facility.

PHYSICAL CHARACTERISTICS

The ordinary shock tube consists of two elongated chambers separated by a burst diaphragm. Initially the gas in one chamber is at a higher pressure than the gas in the other chamber. When the diaphragm ruptures the expansion of the high pressure gas into the low pressure chamber generates a shock wave which travels faster than the expanding gas. Figure 7 shows the pressures and waves in a shock tube. In addition to the compression and expansion chambers and the diaphragm puncturing mechanism, the shock tube system includes a gas supply and regulating system, static pressure and temperature measuring devices and a shock wave velocity measuring system. The shock tube was employed here as a step-function generator for use in the calibration of high frequency pressure transducers. It is an excellent device for this work since it provides a short enough rise time between pressure levels, about 10^{-9} seconds[2], to shock excite transducers having resonances at predominant modes of 100,000 cps and higher.

Physically the two shock tubes of interest here, the prototype tube and the Edwards AFB tube, are very similar. Both were manufactured by the Dresser Dynamics Division of Dresser Industries. Both have uniform cross-section expansion chambers with internal dimensions of 7/8-inch by 1 1/4-inch. Each has a uniform circular cross-section compression chamber. The maximum allowable operating pressure of the compression chamber of each shock tube is 2900 psig. Each is capable of bursting a 2000 psi diaphragm. In both shock tubes the shock wave velocity is measured by timing the interval between output pulses from two blast velocity gages placed a known distance apart along the axis of the expansion chamber. The shock tubes differ in length, the prototype tube having a 4 ft compression chamber and a 19 ft expansion chamber, and the Edwards AFB tube having a 6 ft compression chamber and a 29 ft expansion chamber. They also have different breech-lock mechanisms and gas supply and regulation systems, but these differences are not important as far as the evaluation of the shock tube as a step-function generator is concerned.

THEORETICAL RELATIONS

Consider right traveling shocks as in Figure 7. The velocity of the shock relative to the gas into which it moves is $U-u_1$, and relative to the gas out of which it moves is $U-u_2$. The flow through a shock discontinuity may be treated as though the flow were steady at each instant of time, and the relations for steady-flow normal shocks may be applied if the coordinate system moves with the shock[3, p 995]. The following basic equations are taken from Shapiro[3], Chapter 25, where detailed derivations are presented. The plus sign refers to a right-traveling and the minus sign to a left-traveling shock wave. Shock wave pressure (Shapiro equation 25.23, p 1002)

$$\frac{p_2}{p_1} = 1 + \frac{2\gamma}{\gamma+1}\left[\left(\frac{U-u_1}{a_1}\right)^2 - 1\right] = 1 + \frac{2\gamma}{\gamma+1}\left(M^2-1\right) \tag{1}$$

Relation between particle velocity and velocity of sound (Shapiro equation 24.20, p 945)

$$\frac{a_2}{a_1} = 1 \pm \frac{\gamma-1}{2}\left(\frac{u_2 - u_1}{a_1}\right) \tag{2}$$

Contact surface velocity (Shapiro equation 25.32c, p 1008)

$$\frac{u_2}{a_1} = \frac{\frac{p_2}{p_1} - 1}{\gamma\left[1 + \frac{\gamma+1}{2\gamma}\left(\frac{p_2}{p_1} - 1\right)\right]^{1/2}} \tag{3}$$

Relation between reflected and incident shock (Shapiro equation 25.35, p 1020)

$$\frac{p_5}{p_2} = \frac{\left(1 + 2\,\frac{\gamma-1}{\gamma+1}\right)\frac{p_2}{p_1} - \frac{\gamma+1}{\gamma-1}}{\frac{\gamma-1}{\gamma+1}\,\frac{p_2}{p_1} + 1} \tag{4}$$

Relation between incident and reflected pressure step (Shapiro equation 25.36, p 1021)

$$\frac{p_5 - p_2}{p_2 - p_1} = \frac{\frac{2\gamma}{\gamma+1}}{\frac{p_1}{p_2} + \frac{\gamma-1}{\gamma+1}} \tag{5}$$

These basic relations can be combined and refined to make a set of more useful equations. Assuming that $\gamma = 1.4$ for air, which is reasonable at ordinary temperatues, and that $u_1 = 0$, equation (1) becomes

$$\frac{p_2}{p_1} = 1 + \frac{7}{6}\left[\left(\frac{U}{a}\right)^2 - 1\right] \tag{6}$$

This may be solved for velocity in terms of pressure step, which is

$$U = a\left[\frac{6}{7}\left(\frac{p_2}{p_1} - 1\right) + 1\right]^{1/2} \tag{7}$$

Since the shock wave moves through the medium initially in the expansion chamber, equations (6) and (7) are applicable to both air-to-air and helium-to-air shock tubes. The relationship between the compression-expansion chamber ratio to the shock-wave pressure is developed as follows. The assumptions are made that: (1) the working fluids behave as perfect gases, (2) the entire process is adiabatic, (3) the working fluids are non-viscous, (4) the rupture disc is removed instantaneously and completely, and (5) the specific heats are constant. Consider equation (2) for a rarefaction wave moving leftward into region (3) at the velocity of the region (4) front. In this case γ is the ratio of specific heats for the gas in the compression chamber and $u_3=0$. Assume that the isentropic relation between a and p applies.

$$\frac{p}{p_1} = \left(\frac{a}{a_1}\right)^{\frac{2\gamma}{\gamma-1}}$$

Then

$$\frac{u_4}{a_3} = \frac{2}{\gamma-1}\left(1 - \frac{a_4}{a_3}\right) = \frac{2}{\gamma-1}\left[1 - \left(\frac{p_4}{p_3}\right)^{\frac{\gamma-1}{2\gamma}}\right] \tag{8}$$

But $u_4 = u_2$ and $p_4 = p_2$. Therefore

$$\frac{u_2}{a_3} = \frac{2}{\gamma - 1}\left[1 - \left(\frac{p_2}{p_1}\right)^{\frac{\gamma-1}{2\gamma}}\left(\frac{p_1}{p_3}\right)^{\frac{\gamma-1}{2\gamma}}\right]$$

Combine the above equation with equation (3) and solve for p_1/p_3. The result is

$$\frac{p_1}{p_3} = \frac{p_1}{p_2}\left\{1 - \frac{a_1\left(\gamma_3 - 1\right)\left(\frac{p_2}{p_1} - 1\right)}{2a_3\gamma_1\left[1 + \frac{\gamma_1 + 1}{2\gamma_1}\left(\frac{p_2}{p_1} - 1\right)\right]^{1/2}}\right\}^{\frac{2\gamma_3}{\gamma_3 - 1}} \tag{9}$$

If the same gas is present at the same temperature in both the compression and expansion chambers, $\gamma_3 = \gamma_1$, and $a_3 = a_1$

$$\frac{p_1}{p_3} = \frac{p_1}{p_2}\left\{1 - \frac{\gamma - 1}{2\gamma}\,\frac{\frac{p_2}{p_1} - 1}{\left[1 + \frac{\gamma + 1}{2\gamma}\left(\frac{p_2}{p_1} - 1\right)\right]^{1/2}}\right\}^{\frac{2\gamma}{\gamma - 1}} \tag{10}$$

Assuming air in both chambers with $\gamma = 1.4$, this becomes

$$\frac{p_3}{p_1} = \frac{p_2/p_1}{\left\{1 - \left(\frac{p_2}{p_1} - 1\right)\left[49 + 42\left(\frac{p_2}{p_1} - 1\right)\right]^{-1/2}\right\}^7} \tag{11}$$

For helium-to-air, assuming the helium ratio of specific heats, γ_3 is 1.67, equation (9) becomes

$$\frac{p_3}{p_1} = \frac{p_2/p_1}{\left\{1 - \frac{a_1}{a_3}\ \frac{5}{21}\left(\frac{p_2}{p_1} - 1\right)\left[1 + \frac{6}{7}\left(\frac{p_2}{p_1} - 1\right)\right]^{-1/2}\right\}^5} \tag{12}$$

Equations (11) and (12) are plotted in Figure 8. If the temperature of the two chambers is assumed to be the same, and the velocity of sound is computed assuming perfect gases

$$\frac{p_3}{p_1} = \frac{p_2/p_1}{\left\{1 - \left(\frac{p_2}{p_1} - 1\right)\left[150.4 + 128.7\left(\frac{p_2}{p_1} - 1\right)\right]^{-1/2}\right\}^5} \tag{13}$$

Another useful equation for this work is the relation between reflected pressure and shock-wave velocity. In order to derive this relation consider equation (5) written for air in the expansion chamber with $\gamma = 1.4$. This is

$$\frac{p_5 - p_2}{p_2 - p_1} = \frac{7p_2}{6p_1 + p_2} \tag{14}$$

Add $\frac{p_2 - p_1}{p_2 - p_1}$ to both sides of equation (14) and rearrange

$$\frac{p_5 - p_1}{p_2 - p_1} = 2\left[\frac{7p_1 + 4(p_2 - p_1)}{7p_1 + (p_2 - p_1)}\right] \tag{15}$$

Combining equation (6) with equation (15) yields a more convenient relation

$$\frac{p_5 - p_1}{p_1} = \frac{7}{3}\ (M^2 - 1)\left[\frac{2 + 4M^2}{5 + M^2}\right] \tag{16}$$

This may also be wirtten

$$\frac{p_5}{p_1} = 1 + \frac{7}{3}\ (M^2 - 1)\left[\frac{2 + 4M^2}{5 + M^2}\right] \tag{17}$$

The equations given here include all of those required in shock-tube design and shock-tube experiment evaluation, except those relating to the determination of the pressure-step duration. Reference (5) treats that subject at length.

DESIGN CRITERIA

The primary objective in the design of a shock tube as a device for pressure transducer calibration is to provide an instantaneous pressure step which holds constant at the higher pressure level for several milliseconds. The magnitube of the maximum pressure step determines the upper limit of the range through which gages can be calibrated, so a large step is desirable. Since a normally reflected shock wave has over twice the strength of its incident wave[4], the largest pressure step can be applied to a gage located in the end plate of the shock tube. Of course there are situations where a side port location more nearly reproduces actual conditions, and thus is more desirable than the end plate location. Since the transfer function is a characteristic of the gage and does not depend on the input applied, either gage location could be used. The end plate location is normally the better choice because it allows larger pressure steps, and because the shock front is parallel to the face of the gage. The shock front makes contact with the entire face of the transducer at the same moment and hence the input approaches a true step. Both the Edwards AFB tube and the prototype tube have provisions for both end plate and side port gage location.

In order to obtain as large a pressure step as possible without damaging the gage under consideration, it is necessary to lower the initial expansion chamber pressure. This is because there is a limit to the total pressure the gage can withstand, and the total pressure is equal to the initial expansion chamber pressure plus the pressure step. To achieve a given total pressure after lowering p_1 it is necessary to increase the shock strength. This in turn means increasing the compression chamber pressure, p_3 . Of course, in the actual case there is a limit to the pressure the compression chamber can withstand. This means that complete freedom does not exist in designing gage tests. More explicitly, it is not always possible to impose on a gage a pressure step of 0 psig to full scale. Instead a compromise has to be made between initial expansion chamber pressure and shock strength, so that the desired total pressure may be applied to the test gage. It is desirable to use a low shock strength in gage testing because a high shock strength is characterized by a gradually rising pressure behind the shock front instead of a step.

The time interval during which the constant-pressure exists at the end plate is a function of the gases used in the two chambers, the lengths of the chambers, and the shock strength. A constant-pressure time interval of 10 milliseconds following the shock wave is often sought in shock-tube design[5, p 1]. What is required is that the step be of sufficient duration to permit the recording of enough information to establish the transfer function.

The shock-tube design problem is one of obtaining "a compromise between maximum pressure, maximum-pressure step for a particular gage rating (high shock strength), and chamber lengths".[5, p 3] Here the problem was to evaluate two shock tubes which were already in operation.

In evaluating these two shock tubes, it was immediately obvious (from their maximum pressure level of 2900 psig) that it would be impossible to test over full scale a pressure transducer more than about 1500 psi rating. This is not a severe limitation because the transfer function is invariant with regard to pressure level provided the gage is linear. Linearity should be determined prior to dynamic calibration with a static or psuedo-static calibration device. A non-linear gage does not have a desirable transfer function, and the methods described in this report cannot be used for such gages.

The next step in the evaluation of these two shock tubes was to determine whether or not they have proper physical dimensions. Since the primary consideration in determining shock tube lengths is providing an adequate constant-pressure time interval, this time interval was used as a basis for evaluation. Using a shock strength of $p_2/p_1=2$ and the lengths of the actual sections, the theoretical design relations were applied to each of the shock tubes. This analysis was similar to that given by Wolfe[5]. The resulting constant-pressure time intervals were 5.5 milliseconds for the prototype tube and 8 milliseconds for the Edwards AFB tube. These are considered to be adequate constant-pressure time intervals for reasons which will be given later in the section on the recording equipment.

Thus from a theoretical standpoint the prototype and the Edwards AFB shock tubes are similar, and are adequate for dynamic calibration of pressure transducers.

EXPERIMENTAL RESULTS

Experiments were made on the prototype tube to determine how nearly the actual flow compares with the theoretical. The first characteristic of the actual shock-tube behavior investigated was that of shock-wave velocity attenuation. Figure 9 shows experimental and theoretical velocities versus distance for four values of p_3/p_1. It is apparent that the theoretical relations given by equations (7) and (11) do not accurately predict the velocity in the prototype shock tube. Equation (11) is based on the assumptions of ideal and complete removal of the rupture disc and non-viscous flow. Figure 9 shows clearly that neither of these assumptions is valid. First, it is apparent that if shock velocity is extrapolated back to the zone where the shock formed, the velocity would be lower than the theoretical. This indicates that energy was lost in the diaphragm burst. Next, the non-viscous flow assumption is obviously invalid as demonstrated by the further decrease in velocity.

Equation (7) is based on the assumptions that air obeys the perfect gas law, that the specific heats of the gas are constant, and that the process is

adiabatic. At the temperatures and pressures encountered in the prototype shock tube the first two of these assumptions should be valid. The third assumption should be valid because of the rapid rate at which the process proceeds. Equation (7) has been found valid within experimental uncertainties by several investigators[6, 7]. Since equation (7) is highly accurate, it was used to calculate shock front amplitudes corresponding to the velocities on the attenuation curves given in Figure 9. It was found that a 13.7 psi shock front had an attenuation of 0.51 psi/ft at a point 72 inches from the burst diaphragm. Since shock tube parameters such as hydraulic radius, surface roughness and length all affect the attenuation, experimental determinations should be made for individual tubes. The prototype shock tube and the Edwards AFB tube are constructed of the same material and have the same cross-sectional area and hence should have similar attenuation characteristics.

Equation (11) is often plotted and presented for use in planning tests, Figure 8. However, this relationship is of little value in predicting behavior in tubes which have a large amount of attenuation, as has been shown. For planning tests with a shock tube having a large amount of attenuation, a better approach is to use a calibration curve for the particular shock tube giving actual pressure (as determined from velocity) as a function of p_3 and p_1. Figure 10 is such a curve for the Edwards AFB shock tube. It gives absolute reflected pressure, p_5, plotted against initial expansion chamber pressure, p_1, with initial compression pressure as the parameter. For a given value of p_3/p_1, this reduces to the simple mathematical relation $p_5 = A\, p_1$. In the case where $p_3/p_1=4$, the experimental relation is $p_5=2.2\, p_1$. Since a single pressure ratio, p_3/p_1, is often used for all tests with a particular tube, a relation of this form can greatly simplify planning.

Experiments were also made to determine the actual length of the constant-pressure time interval at the end plate. This was done by photographing the response of a pressure transducer on an oscilloscope. For a compression chamber to expansion chamber pressure ratio of $p_3/p_1=4$, the constant-pressure time interval was found to be 7 milliseconds. This compares to 8 milliseconds predicted by idealized theory.

While the accuracy of equation (17) has not been extensively investigated, Smith and Lederer of NBS found correlation between predicted and experimental result good. Equation (17) would be expected to be accurate because it is derived from equation (7). In addition tests were made to confirm its accuracy. The transducer used in these tests was a Norwood Model 101, which is of the strain gage type. First it was statically calibrated with a dead weight tester. The maximum error was 0.4% of full scale. Then it was dynamically tested in the end plate of the shock tube. The response of the transducer to the shock front was photographed as it was traced on a Tektronix scope. The sweep time of the scope was set so that the pressure step was clearly discernible after the transducer's ringing had ceased. Velocity of the shock front was determined by measuring the time between the responses of two Atlantic Research Blast Velocity Gages placed 6 inches apart, just upstream from the end of the tube.

The amplitude of the dynamic pressure step was then determined from equation (17) and from the measurement of the recorded pressure step and the static calibration. Figure 11 shows the gage's indicated pressure, p_5, plotted against actual pressure for both static and dynamic calibration. The pressure determined from equation (17) was used as the actual pressure for the dynamic test points. The maximum deviation is 2.8% of full scale. This is within the range of maximum probable error of about 5%. The error is composed of two parts: (1) the error in measuring the step amplitude on the photograph (estimated to be 2.5%); and (2) the maximum probable error in pressure step amplitude determination from equation (17), including error in velocity, temperature, and static pressure measurement (estimated to be 2.5%). From the results shown in Figure 11 it can be concluded that the Norwood Model 101 Transducer is linear to both static and dynamic inputs. It may also be concluded that equation (17) provides pressure step amplitudes which are accurate within the experimental uncertainty.

Three other available transducer systems were also put into operation in this work. These were the Kistler, Endevco, and Elastronics systems, which use gages of the piezoelectric type. An accurate static calibration of these gages could not be obtained on available equipment, so they were not used in the pressure step amplitude determination tests.

A lightweight shock tube may be excited into resonance by the shock wave. Acceleration of the tube is transmitted to the transducer which may act as an accelerometer. The response, if any, to acceleration is added to the response to the pressure step. Each gage was tested for this effect by placing a blind flange on the end of the shock tube and mounting the test gage behind it. Thus the gage was isolated from the shock front, but not from the acceleration caused by the force of the front on the end plate. The piezoelectric gages were found to be much more sensitive to the acceleration than the Norwood gage. Acceleration sensitivity could be an important characteristic in the selection of gages, and so it should be investigated in the course of any calibration. In order to make a good dynamic calibration of an acceleration sensitive test gage, it would be necessary to eliminate acceleration effects. This can be done by increasing the mass of the shock tube, which would reduce acceleration in accordance with Newton's second law. An alternative would be to specify limits of sensitivity to acceleration and reject gages which do not meet the specifications.

MAJOR PROBLEMS

The major problems encountered in the shock tube studies were of a mechanical nature. A primary problem encountered was air leakage from the prototype shock tube compression chamber and from the associated air supply tubing. After considerable effort most of these leaks were located and eliminated. A major time delay occurred when one of the Atlantic Research Blast Gages used in shock front velocity determination became inoperative. Three weeks were required to obtain a new Blast Gage.

CONCLUSIONS AND RECOMMENDATIONS

The following modifications were made on the prototype shock tube.

(1) Thermometers were mounted at three locations along the expansion chamber wall, Figure 12. These thermometers were needed to obtain the temperature gradient along the wall, and to provide an accurate temperature for use in acoustic velocity computations.

(2) A low range pressure gage was placed on the expansion chamber to provide an accurate static pressure for use in the pressure step amplitude computation.

(3) The shock tube support system was firmly secured to the floor of the laboratory. The primary purpose was to prevent the tube from being inadvertently displaced from normal alignment, especially during the replacement of ruptured diaphragms. It was thought that this might also reduce the vibration and acceleration effects which are included in the output of the piezoelectric transducers, but no such reduction was observed.

(4) A diaphragm holder to facilitiate the placement of rupture discs was installed in the shock tube. This modification made it unnecessary to use a light layer of grease on the diaphragm to hold it in place while the breech mechanism is being closed. The use of grease was unsatisfactory because it was blown down the tube. This made frequent cleaning necessary.

The addition of three thermometers along the expansion chamber was the only modification made to the Edwards AFB tube. Also, it is recommended that the end plate be bolted to the flange behind the velocity gage ports during tests with the test gage in the end plate. This increases the accuracy of the pressure step determination and has no significant effect on the length of the constant-pressure time interval. Only a small portion of that time interval is recorded during gage calibration. Of course, end plate tests must be used for determination of transducer characteristics with the computer program given in this report.

It is concluded that the present shock tube at Edwards AFB is adequate for use in transducer calibration. Major modifications to the present system, such as replacing the present tube with one more massive and having a larger cross-sectional area or improving the shock-wave velocity measurement technique, are not justified at present. It is recommended that further efforts be concentrated on determining the effect of temperature on pressure transducer characteristics. If a major modification of the facility should result, the above modifications in shock tube size might be feasible.

HIGH TEMPERATURE CALIBRATION

Current calibration methods provide for determination of the transducer transfer function at ambient temperature. But the transducers are often used at elevated temperatures where the characteristics differ from the characteristics at ambient temperature. The sensitivity of pressure transducers to temperature change should be investigated and, if the sensitivity is substantial, a technique for calibration at elevated temperatures should be developed.

NEED Both the electrical and mechanical components of pressure transducers are sensitive to temperature. For this reason, it would be expected that a calibration at room temperature would not be valid at elevated temperatures. The amount of error would, of course, depend both on the temperature level and the transducer design. Pressure transducers which are flush mounted in rocket combustion chamber walls often experience diaphragm temperatures as high as 1200 F in normal operation. An investigation is needed to determine the magnitude of the error introduced by using the ambient temperature calibration on data obtained at elevated temperatures. If the magnitude of the error is large, a high temperature calibration technique should be developed.

PROPOSED SOLUTION The effect of temperature change on response characteristics for several types of transducers should be studied in the following manner. First, analytical studies should be made to estimate the effect of temperature on piezoelectric, strain-gage, and capacitance transducers. Sample gages of each type would then be chosen, and the response characteristics of each type obtained experimentally at various temperature levels. These experiments should be carried out in as simple a manner as possible, with a minimum of special equipment. This means that a precise high temperature calibration would not be obtained, but that is not needed. A comparison between the predicted temperature effects and the actual effects, and an evaluation of the error resulting from the use of an ambient temperature calibration on data obtained at high temperatures would determine the need for high temperature calibration. It would indicate the level of uncertainty which is accepted when a transducer calibrated at ambient temperature is used at a higher temperature. It would show which type or types of transducers are best suited for high temperature operation. It would also show how much additional cooling is required for transducers in rocket test applications to reduce the uncertainty of results to acceptable levels. If the uncertainty for all types of transducers is too high when used in high temperature regions, and the possibility of increased cooling is low, the evaluation would provide evidence that high temperature calibration is needed.

SECTION 3 MATHEMATICAL ANALYSIS AND COMPUTER PROGRAMS

PROBLEM DEFINITION

The two basic objectives for the work performed under this category were to determine feasible and accurate numerical methods for computing (1) the transfer function for any arbitrary transducer system from a known input and output time function, and (2) the input time function for any arbitrary transducer system from a known transfer function and output time function. The primary effort during the first phase of the project was concerned with meeting the first objective. The second objective was subsequently achieved, within limited feasibility conditions.

The block diagram for a typical transducer system is shown in Figure 13. The input time function, $f(t)$, is operated on by the system function, $h(t)$ to obtain the output time function, $x(t)$. If the system's structure is not explicitly known, $h(t)$ is not easily obtained by direct methods and it is necessary to transform the problem from the time domain to the complex frequency domain. This is done by evaluating

$$F(s) = \int_0^\infty f(t)e^{-st}\,dt = \lim_{\substack{T\to\infty \\ \epsilon\to 0}} \int_\epsilon^T f(t)e^{-st}\,dt \tag{18}$$

$$X(s) = \int_0^\infty x(t)e^{-st}\,dt = \lim_{\substack{T\to\infty \\ \epsilon\to 0}} \int_\epsilon^T x(t)e^{-st}\,dt \tag{19}$$

These transformations are based on the assumption that $f(t)$ and $x(t)$ are zero for $t<0$. If the variable, s, is defined as

$$s = \sigma + j\omega \qquad \sigma>0 \tag{20}$$

then the transforms are unilateral Laplace transforms and the time functions are transformed into the complex frequency domain. If the variable, s, is defined as

$$s = j\omega \tag{21}$$

then the transforms are unilateral Fourier transforms and the time functions are transformed into the frequency domain. In either the complex frequency or the

frequency domain, the transfer function is defined as

$$H(s) = \frac{X(s)}{F(s)} \tag{22}$$

The Fourier transform is the better tool for handling time functions with the characteristic that they become zero as $T \to \infty$. Some time functions do not satisfy this criteria, e.g., the step function. However, it is possible to treat this function with the Laplace transform where $s = \sigma + j\omega$ and to consider its limit as $\sigma \to 0$ to be the Fourier transform. The unit impulse, $u_0(t)$ is the best input function for obtaining a system's transfer function since its Fourier transform is

$$F(j\omega) = \int_0^{\infty} u_0(t) e^{-j\omega t} dt = 1 \tag{23}$$

and the Fourier transform of the output is identically the transfer function.

$$H(j\omega) = \frac{X(j\omega)}{1} = X(j\omega) \tag{24}$$

Unfortunately, it is not easy to generate the exact form of a unit pressure impulse. However such functions can be approximated by generating pulses of short duration and large amplitude relative to the parameters of the transducer system being investigated. A number of problems inherent in other methods for determining $H(j\omega)$ would disappear under this approach.

OBTAINING THE SYSTEM TRANSFER FUNCTION

The only feasible alternative for exciting the transducer system is to apply a known pressure step to the system, as is done with a shock tube. As previously indicated, the step function does not have a Fourier transform. If we consider the Laplace transform of the step, then

$$F_{-1}(s) = \lim_{\substack{T \to \infty \\ \epsilon \to 0}} \int_{\epsilon}^{T} u_{-1}(t) e^{-st} dt = \lim_{\substack{T \to \infty \\ \epsilon \to 0}} \left(\frac{1}{s} e^{-s\epsilon} - e^{-sT} \right) \tag{25}$$

Making the substitution $s = \sigma + j\omega$, we obtain

$$F_{-1}(\sigma+j\omega) = \lim_{\substack{T\to\infty \\ \epsilon\to 0}} \frac{1}{\sigma+j\omega} \left(e^{-\sigma\epsilon} e^{-j\omega\epsilon} - e^{-\sigma T} e^{-j\omega T} \right) \tag{26}$$

which becomes for $\sigma > 0$

$$F_{-1}(\sigma+j\omega) = \frac{1}{\sigma+j\omega} (1-0) = \frac{1}{\sigma+j\omega} \tag{27}$$

If $\sigma \ll \omega$, then equation (27) may be approximated by

$$F_{-1}(\sigma+j\omega) = \frac{1}{j\omega} = \frac{1}{\omega} \angle -90^{\circ} \tag{28}$$

Figure 14 shows a typical step function of amplitude A_N , divided into equal time intervals of width Δt . Multiplying the function by e^{-st} yields a new function, $A_N e^{-st}$. The integral of the function may be approximated by evaluating the limit of the sum

$$\lim_{T\to\infty} A_N \sum_{n=0}^{T-1} e^{-sn\Delta t} \Delta t \tag{29}$$

where n is the index corresponding to a sample taken at time, $t = n\Delta t$. Each term in the sum corresponds to a rectangle of area, $e^{-sn\Delta t}\Delta t$. Taking the sum from $n = 0$ to $n = T-1$ implies that each rectangle's area is determined by the area to the right of the index. The limit of this sum is not readily evaluated. A more convenient equivalent form is

$$\lim_{T\to\infty} A_N \sum_{n=1}^{T} e^{-sn\Delta t} \Delta t \tag{30}$$

This form implies that each rectangle's area is determined by the area to the left of the index. The sum is a geometric series and the function may be written in closed form as

$$F(s) \cong A_N \Delta t \; \frac{e^{-s\Delta t}}{1-e^{-s\Delta t}} \tag{31}$$

Multiplying numerator and denominator by $(1+e^{s\Delta t})$, we obtain

$$F(s) \cong A_N \Delta t \left(\frac{e^{-s\Delta t} + 1}{e^{s\Delta t} - e^{-s\Delta t}} \right) \tag{32}$$

Since $s = \sigma + j\omega$, and we desire that $\sigma \longrightarrow 0$, the function may be written

$$F(j\omega) \cong A_N \Delta t \left(\frac{e^{-j\omega\Delta t} + 1}{e^{j\omega\Delta t} - e^{-j\omega\Delta t}} \right) \tag{33}$$

Making the substitutions, $\omega\Delta t = \theta$, and $e^{\pm j\theta} = \cos\theta \pm j \sin\theta$, the function becomes

$$F(j\omega) \cong \frac{-A_N \Delta t}{2} \left(1 + j \operatorname{ctn} \frac{\theta}{2} \right) \tag{34}$$

$$F(j\omega) \cong \frac{A_N \Delta t}{2 \sin \frac{\theta}{2}} \angle - \left(90^\circ + \frac{\theta}{2} \right) \tag{35}$$

Equation (35) gives better results if the transfer function is being computed.

Consider the typical output waveform shown in Figure 15. The Laplace transform of this function may be expressed as

$$X(s) = \int_0^{\tau} x(t) e^{-st} dt + A_N \int_{\tau}^{\infty} e^{-st} dt \tag{36}$$

Where $\tau = N\Delta t$

The second integral can be approximated by the sum

$$A_N \Delta t \sum_{N+1}^{\infty} e^{-ns\Delta t} \tag{37}$$

which can be written in closed form as

$$A_N \Delta t \left(\frac{e^{-(N+1)s\Delta t}}{1-e^{-s\Delta t}} \right) \tag{38}$$

The limit of the expression as $\sigma \longrightarrow 0$ becomes

$$A_N \Delta t \ \frac{e^{-j(N+1)\theta}}{1-e^{-j\theta}} \quad \text{where } \theta = \omega \Delta t \tag{39}$$

Expanding and collecting real and imaginary parts yields

$$A_N \int_{\tau}^{\infty} e^{-st} dt = \frac{-A_N \Delta t}{2} \left[\cos N\theta + \sin N\theta \cdot \operatorname{ctn} \frac{\theta}{2} + j \left(\cos N\theta \cdot \operatorname{ctn} \frac{\theta}{2} - \sin N\theta \right) \right]$$

$$= \frac{-A_N \Delta t}{2 \sin \frac{\theta}{2}} \left(\sin (N+\tfrac{1}{2}) \theta + j \cos (N+\tfrac{1}{2}) \theta \right) \tag{40}$$

For a given waveform sampled at N points separated by uniform intervals of Δt, this equation will be a constant at any value of ω. Because of the upper limit of infinity, it is not possible to numerically integrate the left-hand side of equation (40). However, the right-hand side can be easily computed for any value of $\frac{\omega \Delta t}{2}$ that is not 0 or an integral multiple of π.

The first integral in equation (36) is finite and can be computed by several numerical methods. The integral is

$$\int_0^{\tau} x(t)\ e^{-st} dt \tag{41}$$

Since τ is finite, the limit as $\sigma \longrightarrow 0$ is finite and the integral becomes

$$\int_0^{\tau} x(t) e^{-j\omega t} dt \tag{42}$$

which can be written in the form

$$\int_0^T x(t)\cos \omega t \, dt - j\int_0^T x(t)\sin \omega t \, dt \tag{43}$$

The sum of the real parts of equations (40) and (43) is real and is

$$R = \int_0^T x(t)\cos \omega t \, dt - \frac{A_N \Delta t}{2 \sin \frac{\theta}{2}} \sin\left(N+\tfrac{1}{2}\right)\theta \tag{44}$$

The sum of the imaginary parts of equations (40) and (43) is imaginary and is

$$I = -\left[\int_0^T x(t)\sin \omega t \, dt + \frac{A_N \Delta t}{2 \sin \frac{\theta}{2}} \cos\left(N+\tfrac{1}{2}\right)\theta \right] \tag{45}$$

The Bowersox[1] approximation for the integrals in equations (44) and (45) are

$$\int_0^T x(t)\cos \omega t \, dt \cong \Delta t \sum_{n=1}^{N} A_n \cos n\theta \tag{46}$$

and

$$\int_0^T x(t)\sin \omega t \, dt = \Delta t \sum_{n=1}^{N} A_n \sin n\theta \tag{47}$$

Any numerical approximation for the two integrals will be of a product form with one of the factors being the sampling interval, Δt . Since Δt will be common to all of the terms in the approximation to $X(j\omega)$, $X(j\omega)$ can be written in the form

$$X(j\omega) = (X + jY)\ \Delta t = \left(\frac{R}{\Delta t} + j\,\frac{I}{\Delta t}\right)\Delta t \tag{48}$$

The transfer function can then be expressed as the ratio, $\frac{X(j\omega)}{F(j\omega)}$. Substitution of the approximations of equations (35) and (48) gives

$$H(j\omega) \cong \frac{(X + jY)\ \Delta t}{\frac{A_N \Delta t}{2 \sin \theta/2}\ \Big/ -\left(90^\circ + \frac{\theta}{2}\right)} \tag{49}$$

$$H(j\omega) \cong \frac{2 \sin \frac{\theta}{2} \sqrt{X^2 + Y^2}}{A_N}\ \Big/ \tan^{-1} Y/X + 90^\circ + \theta/2 \tag{50}$$

In numerically evaluating equation (50) several important factors must be considered:

(1) The sampling interval, Δt , must be factored out of the numerical approximation to the integrals in equations (44) and (45), i.e., $X = R/\Delta t$ and $Y = I/\Delta t$.

(2) The phase computation must evaluate the signs of X and Y in order to locate $\tan^{-1}(Y/X)$ in the correct quadrant.

(3) The angle, $\theta/2 = \omega\Delta t/2$, cannot be zero or an integral multiple of π.

(4) The accuracy of the computation is determined by Δt . The Sampling Theorem dictates that ω not exceed $\pi/\Delta t$. At $\omega = \pi/\Delta t$, θ will be 180° .

(5) The point for the upper limit of integration should be carefully chosen. For best accuracy, the point should be at an amplitude which is the same as the limiting value and where the damped sinusoids have reached approximately 99% of their final value.

A point often neglected by those concerned with the Sampling Theorem is the error introduced by the presence of frequencies in excess of the theoretical limit of $f_{max} = 1/2\ \Delta t$. If such frequencies are present in the sampled waveform, their presence will introduce errors in the values computed for frequency components less than f_{max} .

COMPUTATION OF TRANSFER FUNCTIONS

Bowersox and Carlson[1] reported excellent results in approximating the amplitude characteristic of the transfer function for a known single-degree-of freedom transducer. However, poor results were obtained in approximating the phase characteristic. The example considered had a natural frequency of 500 cps. Their sampling frequency was apparently 5000 cps.*

In order to investigate the problems encountered by Bowersox and Carlson, several computer programs were written in the Illiad language (a one-pass compiler for the IBM 650). These programs were:

(1) A program which computes the ordinates for the output time function of a single-degree-of-freedom system as a function of time. This program generates data for the transfer function approximation program.

(2) A program which computes the amplitude and phase characteristic for a known single-degree-of-freedom transfer function as a function of frequency. This program provides data for comparison with the approximated transfer function.

(3) A program which computes the transfer function from any arbitrary time response data which corresponds to a step input. This program is similar to the Fortran program provided by the Air Force. It includes an arctan function which computes the angle and locates the result in the proper quadrant.

These Illiad programs were run on the IBM 650 at the University of Houston. Bowersox and Carlson's results including the phase discrepancy, were reproduced in order to verify the programs.

Extensive analysis of the relationships used in the program did not lead to an explanation for the large error in phase characteristic. However, it was noted that small errors in the values computed for X and Y in equation (50) will tend to have greater significance in the phase calculation, due to the nature of the arctan function commonly utilized in computer programs.

This function is a polynomial approximation to the arctan curve. The variable of the polynomial is

$$Q = \frac{|Y/X| - 1}{|Y/X| + 1} \tag{51}$$

* Several typographical errors appear in the Bowersox-Carlson report.

and will always be in the range $-1 \leq Q \neq 1$.

$$P(Q) = C_o + \sum_{i=0}^{6} (-1)^i C_k \cdot Q^k \quad \text{where} \quad k = 2i + 1 \tag{52}$$

An error in $|Y/X|$ will induce an error in Q which will induce an error in $P(Q)$. A somewhat complicated error function results from an analytical approach to the error analysis of this function. An example will better illustrate the significance of erroneous values for Y and X . The maximum error in $|Y/X|$ occurs when the error increases Y and decreases X or vice versa. Hence, the worst case for a 5% error in each would yield the expression

$$Q' = \frac{1.1\,|Y/X| - 1}{1.1\,|Y/X| + 1} \tag{53}$$

If we define the ratio of Q'/Q as r, and replace Q in $P(Q)$ by rQ, then $P(Q)$ becomes

$$P(Q) = C_o + \sum_{i=0}^{6} (-1)^i C_k r^k Q^k \quad \text{where} \quad k = 2i + 1 \tag{54}$$

The effect of the error is to modify the coefficients, C_k , by r^k . It is obvious from equation (53) that errors will tend to cancel out for $|Y/X| \gg 1$, e.g., $Q' = .982$ and $Q = .980$ and $r = 1.002$ when $|Y/X| = 100$. If $|Y/X| = 10$, $Q' = .917$, $Q = .818$ and $r = 1.121$. For the latter case, the coefficients will be increased by approximately 12%, 40%, 75%, 118%, 173%, 241%, and 326% for C_1, C_3 , C_5, C_7, C_9, C_{11}, and C_{13}, respectively. Obviously the phase characteristic will be in substantial error if the $|Y/X|$ value is in error.

The values of X and Y can be computed more accurately by increasing the sampling frequency and/or using a more accurate approximation for the integrals in X and Y . In order to verify this conclusion, the Illiad programs were rewritten in FORTRAN (IBM 7090). The method of integration was not changed. The programs were compiled and run at the Houston CEIR Center.

The transfer function approximation program was supplied with 161 data points from the single-degree-of-freedom example. This corresponded to an increase in sampling frequency to 10,000 cps which is 20 times the natural frequency of the example. The results are shown in Figures 16 and 17. As expected the amplitude characteristic changed insignificantly whereas the phase characteristic improved radically.

The approximate phase characteristic obtained by increasing the sampling frequency to 10,000 cps is displaced by a variable amount which (as learned after considerable investigation) is equivalent to $\theta/2$. Re-evaluation of the analysis does not account for this displacement. If the form of the transfer function is assumed to be

$$H(j\omega) = (X + jY)e^{-j\theta/2}\Delta t \qquad (55)$$

where X and Y are as previously defined, the approximate phase will agree with the exact phase. The effect of this factor is to shift the phase characteristic. The transfer function approximation program was modified to include this factor and the example was rerun. The results obtained for the phase characteristic are also shown in Figure 17. It will be noted that the approximate and exact curves coincide as expected.

Two FORTRAN (7090) programs were written in order to check the two-degree-of-freedom example in Bowersox and Carlson. One of these programs generates the time response data required for input to the transfer function approximation program. The other program evaluates the Bowersox analytic transfer function in order to provide data for comparison. The results obtained from the latter program did not agree with those obtained by the approximation program. Further checking indicated that Bowersox's analytic functions for the two-degree-of-freedom case are not consistent.

A third FORTRAN (7090) program was written. This program utilizes the constants in the time response function for a step input to compute the corresponding transfer function. The data generated by this program corresponds to the exact transfer function.

The approximate and exact amplitude characteristics are shown in Figure 18 and phase characteristics are shown in Figure 19. A sampling frequency of 100,000 cps was utilized in the approximation and 1501 points were sampled. The natural frequencies are approximately 2151 cps and 3775 cps. Excellent agreement also exists in this example.

An investigation of the effect of transient waveform data truncation on the accuracy of the transfer function was conducted. The following criteria have been established for truncating transient waveform data:

(1) The data must be truncated at a point which lies on the positive going edge of a cycle of oscillation.

(2) The data must be truncated at a point which is near the value reached when the oscillations have ceased.

(3) The data must be truncated at a point which will yield an odd number of data points, i.e., an even number of sampling intervals.

The first two criteria tend to minimize the error in the approximate transfer function which is obtained from the truncated data. The third criteria is imposed by Simpson's Rule, which is the basis for the numerical integration performed by the computer programs.

The preceding criteria were applied in obtaining four data sets from the two-degree-of-freedom test case. These four data sets were obtained by truncating the response data at time values in the neighborhood of one, two, three and four times the longer of the two system time constants. The system transfer function was computed for each of the four data sets and the results compared with the known transfer function. The following general conclusions are drawn from this comparison:

(1) The amplitude characteristic is more sensitive to truncation than the phase characteristic.

(2) The maximum error in amplitude characteristic occurs within the frequency range contained by the 3 db points on the peaks associated with the poles of the transfer function.

(3) The minimum phase error occurs at the frequencies corresponding to the poles of the transfer function.

(4) A reasonably accurate transfer function can be obtained with data which has been truncated at a time value near one time constant.

Table I contains the computed amplitude and phase characteristics obtained from each data set at frequencies near the natural frequencies.

On the basis of the results obtained from this investigation, it was concluded that the data can be truncated without significant loss of accuracy in the computed transfer function. This conclusion assumes that the transducer time constants are related to the natural frequencies such that no more than 10 to 15 cycles of oscillation occur within a period equal to twice the longest time constant. Since the system time constants are usually not known, an alternate rule is that the envelope of the oscillation peaks be within 86% of the final value and the leading and trailing edges of the oscillations be no closer than 0.5 centimeters on the CRT display.

The criteria for truncation require that the final value of the transient be known. In general, this value can only be estimated by the user. The computer programs have been organized so that the final value is estimated as the average value of the waveform described by the data, if the user elects to have the program do so. The computed estimated value is compared with the last two input

data points. If the computed estimated value is not bounded by the last two data points, the program discards the last data point and recomputes the average value of the remaining data. The new estimated value is again compared with the last two data points. The process continues until the computed estimated value is bounded by the last two data points.

The final version of the computer program for computation of transfer functions is written in FORTRAN (7090) and contains the following major sections:

(1) Velocity, Mach Number, and Pressure Step Computation

(2) Final Value Computation (As an optional calculation)

(3) Echo Check and Preliminary Output

(4) Transfer Function Computation

Input data cards to the transfer function computation program include:

(1) Heading Information

(2) Approximate Transfer Function (Listing and Cards)

The detailed formats for all output are such that all information is properly identified and is tabulated in a logical and orderly arrangement.

OBTAINING THE INPUT TIME FUNCTION

The mathematical analysis for determining the input time function which corresponds to an arbitrary transducer response is quite similar to the mathematical analysis for determining the transducer transfer function. In fact, the process for transforming the time response, $x(t)$, to the frequency domain is identical to that developed for the preceding case. Hence, the relations stated in equations (44), (45) and (48) hold for the transformations which define $X(j\omega)$, the Fourier transform of $x(t)$. Since the Fourier transform requires that $x(t)$ become zero (or a constant value) as t tends to infinity, it is necessary that the arbitrary time response data satisfy this requirement.

From equation (22) with $s = j\omega$ (i.e., $\sigma = 0$) , we obtain

$$F(j\omega) = \frac{X(j\omega)}{H(j\omega)} \tag{56}$$

This equation states that the Fourier transform of the input time function, $f(t)$, is defined by the ratio of the Fourier transform of the output time function and the transfer function. Since the approximated transfer function is defined at

discrete values of frequency, it is implicit that $X(j\omega)$ be defined at the same values of frequency.

In order to transform the Fourier transform of $f(t)$ back to the time domain, the inverse Fourier transform must be evaluated. This transform is

$$f(t) = \frac{1}{2\pi} \int_{-\infty}^{\infty} F(j\omega) e^{j\omega} d\omega \tag{57}$$

Since $F(j\omega)$ is complex, it can be written as

$$F(j\omega) = A(j\omega) + j\, B(j\omega) \tag{58}$$

Substitution of equation (58) and Euler's relation into equation (57) yields

$$f(t) = \frac{1}{2\pi} \int_{-\infty}^{\infty} \left[A(j\omega) \cos \omega t - B(j\omega) \sin \omega t + j(A(j\omega) \sin \omega t + B(j\omega) \cos \omega t)\right] d\omega \tag{59}$$

Since $f(t)$ is real, the imaginary part of equation (59) is zero. Also, since both terms in the real part of equation (59) are even functions of ω, the range of integration can be cut in half and the result multiplied by two. Hence, the relation for $f(t)$ becomes

$$f(t) = \frac{1}{\pi} \int_{0}^{\infty} \left[A(j\omega) \cos \omega t - B(j\omega) \sin \omega t\right] d\omega \tag{60}$$

Since $f(t)$ is zero for t less than zero and the first and second terms in equation (60) are even and odd functions of time, respectively, $f(t)$ can be determined from either of the relations

$$f(t) = \frac{2}{\pi} \int_{0}^{\infty} A(j\omega) \cos \omega t \, d\omega \tag{61}$$

$$f(t) = \frac{-2}{\pi} \int_{0}^{\infty} B(j\omega) \sin \omega t \, d\omega \tag{62}$$

If it is assumed that the frequency spectrum of $f(t)$ is zero for frequencies in excess of f_u, then the upper limits on equations (61) and (62) become ω_u.

COMPUTATION OF INPUT TIME FUNCTIONS

In order to evaluate numerically the input time function, we must sample its Fourier transform at a rate which is determined by the upper limit assumed for the spectrum of $f(t)$ and the time interval over which we desire to obtain $f(t)$. This criteria is imposed by the alternative form of the well known Sampling Theorem: "Any $2f_uT'$ unique (independent) pieces of information are needed to completely specify a signal over an interval T' seconds long."[7] For example if f_u is 10,000 cps and T' is 1 second, then 20,000 samples of $f(t)$ are required. However, an important implication of the Sampling Theorem is that $2f_uT'$ samples of $F(j\omega)$ are also necessary in order to avoid an effect referred to as "aliasing" in computing technology.[8] "Aliasing" occurs whenever the argument of the sine and cosine functions in equations (50) and (51) assume values at a time, t_2, that differ from the values at a time, t_1, by an integral multiple of π radians, at corresponding frequencies. For example, assume the following values: $t_1 = 0.5$ seconds, $t_2 = 1.0$ seconds, $f_u = 10{,}000$ cps, $\Delta f = 0.5$ cps, and $\omega = (2\pi\Delta f) = \pi$. Then at time t_1, the argument is 90°; and at time t_2, the argument is 180°. If the frequency increment is changed to 1 cps, then at time t_1, the argument is 180°; and at time t_2, the argument is 360°. For the latter case, the results obtained from evaluating the two equations at times t_1 and t_2, respectively, would have the same magnitude and differ only in sign. The results for t_2 or any time greater than t_2 would be completely erroneous.

The only way in which the effect of aliasing can be avoided when samples of equal intervals are being taken is to sample the frequency function, $F(j\omega)$, at intervals of ΔF, such that

$$\Delta F < \frac{1}{2T'} \tag{63}$$

where T' is the longest time period for which $f(t)$ is to be determined. It should be noted that decreasing ΔF leads to substantial increases in computation time.

A rough estimate of the computation time for a function with a spectrum up to 10,000 cps that is to be computed over a 1 second period can be made. The frequency function must be sampled at 20,000 points in order to avoid aliasing and the input time function must be computed at 20,000 points in order to display a 10,000 cps frequency. The computer will have to evaluate a sine function and a cosine function at each of the 20,000 frequency points, therefore a reasonable estimate of the average number of instructions executed per

frequency point is 100. In order to evaluate one point in time, the computer must numerically integrate over the 20,000 frequency points. Hence, the computer executes approximately 2,000,000 instructions in evaluating a single time point. At an average of 12 microseconds per instruction, each time point will require approximately 24 seconds of computation. To evaluate 20,000 time points will require 8,000 minutes or 133 hours of computation.

A knowledge of the frequency spectrum of the input time function can reduce the computation time considerably. For example, if it is known that the amplitude of the higher frequency components of the input time function is much less than that of the lower frequency components, the number of time points computed can be reduced to a value which is twice the known highest frequency component of interest. Similarly, if the output time function does not display higher frequency components, then the upper limit of integration and sampling rate can be reduced. Hence, the computation time of 133 hours might be reduced to several hours through the exercise of judgment.

It is evident that the computation of input time functions can be a costly process since IBM 7090 time is not inexpensive (typical commercial rates are $550.00 per hour).

The Input Time Function Approximation program may be used to compute the input time function from the time response to an arbitrary input and the approximate transfer function of the transducer. The time response must have reached a steady state value in order for the methods in this program to be valid. Input to the program is:

(1) Heading Information

(2) Approximate Transfer Function Cards

(3) Arbitrary Time Response Cards

Output from the program includes:

(1) Echo Check of Input Data

(2) Approximated Input Time Function

The known two-degree-of-freedom system data set was used in verifying the methods incorporated into the Input Time Function Approximation Program. The output time response was sampled at 1501 points over a 15 millisecond interval or at a sampling rate of 100KC. The approximate transfer function was computed over a frequency range from 1 to 5,000 cps in increments of 25 cps. The input time function was approximated over a 15 millisecond interval. Figure 20 shows the output time response, the approximated input time function and the actual input time function.

The input time function can be evaluated for any Fourier transformable function from either equation (61) or equation (62). The program evaluates both equations in order to give some means of testing the validity of results. For a Fourier transformable function, the two results will be the same. However, the step function is not a Fourier transformable function and the results obtained from equation (61) will be approximately zero. The Transfer Function Approximation Program computes the approximate input time function and the results of evaluating equations (61) and (62) appear as output. In general, the results labeled "Input Time Function No 1" should be approximately zero if a true step function was applied to the transducer.

TRANSDUCER COMPENSATOR

Since a pressure transducer is not an all-pass network, an output voltage obtained from it will generally have a different appearance than the pressure variation causing the response. This is particularly true when the input pressure variation contains harmonics of the resonant frequencies of the transducer. A voltage variation which is exactly the same as the pressure variation can be obtained by applying the transducer output to a network which has a transfer function that is the inverse of the transducer's transfer function.

For the purpose of discussion, a single-degree-of-freedom system will be considered. In the Laplace notation, the transfer function of a single-degree-of-freedom pressure transducer is of the form

$$H(s) = \frac{1}{k\left(\frac{s^2}{\omega_n^2} + \frac{2\zeta}{\omega_n}s + 1\right)} \tag{64}$$

$$H(s)^* = k\,H(s) = \frac{1}{\frac{s^2}{\omega_n^2} + \frac{2\zeta}{\omega_n}s + 1} \tag{65}$$

$H(s)^*$ differs from $H(s)$ by only a constant factor k. Thus the inverse function, which we wish to synthesize, ignoring k, is given by:

$$H(s)^{-1} = \frac{s^2}{\omega_n^2} + \frac{2\zeta}{\omega_n}s + 1 \tag{66}$$

There are several possible methods of inverse transfer function simulation.

Passive Network Synthesis. No exact synthesis is possible since $R_e(H(s)^{-1}) < -1$ as $\omega \rightarrow \infty$. An approximation to the required network may be realizable, however it will probably contain many elements. A passive network synthesis is the least desirable solution since adjustment will be difficult and flexibility will be limited.

Solution of Differential Equation. The differential equation describing transducer operation may be solved by analog computer techniques. The computer diagram for such a solution is indicated in Figure 21. Two practical restrictions limit the usefulness of this approach. (1) While this network does realize the exact inverse transform for frequencies at which the operational amplifiers can be considered perfect, it suffers from degradation due to noise. This noise problem was circumvented by simulating the approximate inverse transfer function on an analog computer without employing differentiators. Figure 23 displays the results obtained from this simulation. (2) For higher frequency transducers, practical limitations of operational amplifier design result in substantial error. Employing time scaling techniques allows simulation of these transducers but requires a time scaled input. Thus the transducer signals must be recorded and played back at slower speed. This would substantially increase data reduction time, assuming that the necessary time scaling can be achieved. Time scale factors of 10^4 or greater are required.

Active Network Synthesis. Although the analog computer simulation requires active components, the approach considered here is different. Figure 22 indicates a method to realize the exact inverse of a transfer function. The only requirement is that $kH(s)$ have its zeros confined to the left-half s plane. For the particular $H(s)$ at hand, this is not the case. The system will tend to be unstable. It may be possible to approximate the inverse with sufficient accuracy if stability can be maintained.

Hence, each of the synthesis methods will only approximate the required transfer function. The use of active elements provides the most easily adjusted and flexible networks.

A preliminary investigation of the techniques for simulating inverse transfer functions was made. The analog computer has been used for simulating these techniques. The results of this study indicate that stability and accuracy are opposing factors in techniques which are based on active networks. It appears that the final answer will represent a compromise between active and passive networks.

The impracticality of digital compensation techniques dictates that a solution to the transducer compensation problem must be analog in nature. This

solution will be determined only through a comprehensive and thorough investigation of the problem. It is thought that a solution does exist and it is recommended that a development program be initiated with the following objectives:

(1) Determine a minimum configuration of active and passive elements that will compensate pressure transducers on a real time basis. The analog computer will be utilized as a simulation tool during this phase of the program.

(2) Design and fabricate a prototype of the compensator system determined under the preceding objective.

(3) Modify the digital computer programs such that they determine the parameter settings for the compensator system from the computed transfer function.

CONCLUSIONS

It is concluded that the Fourier transform method is a highly accurate method for determining transfer functions from the time response to a unit step or input time functions from the time response and known transfer function. In addition to data accuracy, the accuracy of an approximation is related to the sampling frequency and the error in the arguments presented to the arctan function. In the case of transfer function approximation, it has been observed that an irregular phase curve characterizes a poor approximation. It is suggested that this be used as a criteria for confidence in the results obtained for a given approximation. An irregular phase characteristic tends to become smooth as the sampling rate is increased. Little improvement in phase characteristic is obtained for sampling rates in excess of twenty times the highest frequency of interest.

It is also concluded that the time response to a step input can be truncated without serious loss of accuracy. The actual error is a function of the point of truncation and the nature of the function being truncated. For a two-degree-of-freedom system, the maximum error in the approximated transfer function was found to be less than 10% when the data was truncated at a point in the neighborhood of 86% of the final value of the waveform. On the basis of experimental results obtained for known functions, it appears that truncation has a greater effect on amplitude than on phase (see Table I).

Due to the severe computation time requirements associated with approximating the input time functions, it is concluded that this is not an economically feasible method for compensating transducer responses. A more desirable method for compensation is one in which the compensator is cascaded with the transducer so that compensation occurs in real time.

The validity of analog computer techniques for transducer compensation was verified. However, the time scaling requirements imposed by this

solution to the problem cannot be practically achieved with existing recording equipment (e.g., scale factors of 10^4). Hence, it is concluded that this method is not feasible.

It is concluded from an analytical investigation of active network methods for compensation that such methods lead to exact compensation. However simulation of these methods on the analog computer indicates that stability problems exist. It appears that a combination of active and passive networks may result in a compensator which is capable of operating in real time and which will be stable. Further research in this direction is required in order to arrive at a feasible technique and network configuration for transducer compensation. Substantial savings will accrue if transducer compensation is performed by analog techniques whereas substantial expenditures will occur if the compensation is performed digitally.

SECTION 4 DATA REDUCTION SYSTEM

DESCRIPTION OF EXISTING EQUIPMENT

A brief description of the units which make up the data reduction system will aid in discussing the operation of that system. The major functional units are:

(1) Tektronix RM-35 Oscilloscope. This unit is utilized both in recording the transient waveform and in scanning the resulting transparency.

(2) Horizontal and Vertical Position Counters. These counters provide a digital record of the position of the flying spot each time it crosses the recorded waveform.

(3) Digital Control Unit. This unit provides timing and control signals for the system.

(4) Flying Spot Scanner Unit. This unit is utilized as a camera mount during the recording phase and as the flying spot detector during the digitizing phase.

(5) Digital Recording Unit. This unit consists of a Hewlett-Packard 560A Digital Recorder and an IBM 523 Summary Punch which provides the ability to record on paper tape and IBM cards, respectively. In addition the digital recorder provides the analog equivalent of the digitized quantities both for monitoring the digitizing process and controlling the horizontal position of the flying spot.

System operation involves two phases, recording and digitizing. During the recording phase, a plug-in vertical amplifier unit is utilized with the RM-35 for obtaining a trace of the transient waveform. This is photographed through the lens system contained in the Flying Spot Scanner Unit. Any calibrating information desired for this waveform must be obtained by photographing precision horizontal and vertical calibrating waveforms on separate transparencies. These can be photographed either before or after the transient waveform is photographed.

The digitizing phase requires the use of a time base generator plug-in unit for the RM-35. The time base generator provides a precision linear sweep voltage for driving the flying spot in the vertical direction at 5 ms/cm. The digitizing process is initiated by placing the transparency of a photographed waveform in the Flying Spot Scanner Unit and resetting the digital control unit. The X and Y counters are simultaneously reset to 000 and 0000 respectively. The digital control unit generates a pulse that drives the X counter to position 001. After a short delay, the output of a 100KC oscillator is permitted to drive

the Y counter. At the same instant the time base generator is triggered and the flying spot begins a vertical sweep. As the flying spot sweeps vertically, the Y counter continues counting at a 100KC rate until the photomultiplier circuit senses that the spot has moved into the waveform trace. At this time, the digital control unit switches a flip-flop between the output of the 100KC oscillator and the input to the Y counter. This reduces the counting rate of the Y counter to 50KC while the spot continues to fall in the waveform trace. Immediately after the photomultiplier detects the spot moving out of the waveform trace, the input to the Y counter is disabled. Hence, this counter holds a digital value proportional to the amplitude of the waveform trace at this X value. A print cycle is now initiated and the contents of the X and Y counters are either printed, punched on IBM cards, or both. At the conclusion of the printing cycle, the digital control unit advances the X counter to the next position and the process is repeated. The half-counting rate of the Y counter during the time the spot is in the waveform trace produces a count which is proportional to the amplitude of the center of the trace at that X position.

SYNCHRONIZATION OF IBM 523 SUMMARY PUNCH Check-out of the system during the first phase of this project disclosed the existence of certain problems which prevented operation consistent with design specifications. The first of these problems was the lack of coordination between the FSADC and the IBM 523 Summary Punch. The digital control unit emits punch commands at fixed time intervals, while the IBM 523 Summary Punch is capable of accepting a punch command only during a certain portion of its cycle of operation. Since the timing systems of the two units were independent, the punch frequently received a punch command when it was not capable of accepting it. With no provision for synchronization, this resulted in erroneous data being punched on the IBM cards.

ERRATIC COUNTER OPERATION WHEN INTERRUPTING DIGITIZING CYCLE The second problem was that the counter would not remain at the same setting when it was restarted after being interrupted. Provision is made in the Data Recording System for stopping and re-starting the digitizing operation at any position of the X counter. This operation should permit continuation of the digitizing cycle from the point at which it was suspended. It was observed that the X counter would advance to a completely different count upon re-starting. Consequently, the digitizing cycle could not be restarted after being interrupted without risk of recording erroneous data.

DRIFT The third problem was that considerable drift occurred in the data produced by the Data Reduction System. A method was devised to pinpoint the major cause of drift. Three sets of data were utilized. Two sets of data were taken by digitizing a transducer output waveform twice in succession. The third set of data was taken by digitizing the same waveform the following day. A tabulation was made of the differences of the output of the Y counter for identical X counter outputs versus the slope of the waveform being digitized. The results are shown in Figures 24 and 25. The points selected for plotting are those for which the slopes determined for each set of data are approximately

equal and maintain equality for a minimum of two consecutive values of X. Figure 24, using data obtained consecutively, clearly shows that the deviation of the digital value is directly proportional to slope. Figure 25, using data obtained on separate days, shows the same result although not as dramatically. Apparently, other factors have affected these results considerably. Nevertheless, these results clearly indicate that a major factor affecting drift is the horizontal flying spot stability. Further investigation revealed that the regulation of the voltage in the Hewlett-Packard 560A Digital Recorder supplying the horizontal positioning voltage is only 0.5%. For the maximum number of total samples (1000), a regulation of 0.1% would be required just to keep the possible voltage variation within the limit of one sampling increment. A regulation of 0.01% would be preferable.

A careful observation of the points of maximum deviation in these three sets of data, some of which were as high as 20%, indicates that all deviations were less than that which could be caused by X-axis shift. Indeed some deviations can be explained only in this way as the vertical repeatability has been found accurate to approximately 0.25%.

The following conditions which might also contribute to drift, or the recording of erroneous data, were observed.

(1) Variation of Photomultiplier Output. When digitizing a waveform transparency, the output of the photomultiplier was observed to vary considerably with both time and the horizontal beam position. The variation with time does not appear to be a particular problem, but variation with horizontal beam position was severe.

(2) Variation in Trace Intensity. Some variation in trace intensity was observed. The causes are varying phosphor emission over the face of the cathode ray tube, varying spot speed, and varying intensity and astigmatism as the spot moves across the face of the tube. The effect of this intensity variation is to vary the detection level of the Flying Spot Scanner, thus reducing system accuracy.

(3) Waveform Resolution. Since the transient waveform is recorded from the face of an oscilloscope CRT, a restricted area is available for viewing the waveform. Recording the entire transient crowds the individual cycles of the waveform so close that they cannot be adequately resolved. On the other hand, increasing the sweep speed to permit proper resolution results in truncation of the transient and information is thus lost.

INTRODUCTION OF CALIBRATING DATA The fourth problem was the lack of calibration data on the transparency along with the transient waveform. To obtain the best results from the system, it is imperative that calibrating data

be recorded with the transient. Otherwise, long term drift in the system can render the recorded waveform almost useless at a later date. One method would be to record the transient, horizontal, and vertical calibrating waveforms on three separate transparencies. A more accurate procedure would place the three waveforms on the same transparency. In addition to placing all required data in the same location, this method would allow increased accuracy for both recording and digitizing. However, the present system does not permit photographing both the transient and calibrating waveforms simultaneously.

SYSTEM WITH MINOR MODIFICATIONS

Since the completion of several minor modifications it is possible to photograph and digitize a transient waveform, print the data on paper tape, and punch the data on IBM cards in a manner suitable for use on the computer. The system is now fully operable. The minor modifications are described in the following paragraphs.

SYNCHRONIZATION OF IBM 523 SUMMARY PUNCH The diode gate circuit shown in Figure 26 was installed and checked out. This circuit functions to prevent clock pulses from advancing the X counter and resetting the Y counter until the card punch has operated. Two counter circuits in the Digital Control Unit were modified to permit maximum operating speed of the Card Punch and the Digital Recorder, Figure 27. The X16 and X4 scalers were modified to X12 and X3 respectively. This modification permits an operating speed of 100 counts per minute. However, when operating the Card Punch, a punching rate of only 40 cards per minute was obtained. It was found that, although the IBM 523 speed is quoted at 100 cards per minute, this rate applies to gang punching or mark-sensing only. The maximum summary punch rate is specified by IBM as 50 cards per minute. Discussions with IBM indicated that a higher punch rate should be possible with minor modification of the punch and the card punch coupler. Modifications were made and tested, but difficulties with relays in both units prevented satisfactory operation. While correction of the difficulty with the Card Punch Coupler appears to be relatively simple, correction of the problems in the IBM 523 seem almost impossible. For this reason the modifications in the IBM 523 and the Card Punch Coupler were removed and the 40 cards per minute rate was accepted as the maximum if major modification were not to be made. This rate is still 7 cards per minute faster than that obtained prior to the counter modifications.

COUNTER OPERATION WHEN INTERRUPTING DIGITIZING CYCLE The erratic counter operation observed on operation of the start and stop switches was investigated and corrected. The cause was found to be a loading change on the decade counter staircase outputs resulting from transients induced on the -200 volt supply by the start and stop switches. Installation of current limiting resistors in the start and stop switch circuits eliminated the transients, Figure 28. The digitizing cycle can now be restarted after interruption without risk of introducing erroneous data points.

PHOTOMULTIPLIER OUTPUT The photomultiplier output was made more uniform by careful alignment of the photomultiplier tube. This plus adherence to the procedure of focusing the spot at the center of the screen made considerable improvement in the operation of the Flying Spot Scanner.

TRANSPARENCY IMPERFECTIONS Careful processing of the film reduces to a minimum the number of flaws in the transparencies. Any major spots are removed by retouching the film with Kodak Opaque.

WAVEFORM RESOLUTION The waveform truncation studies reported in the section on Mathematical Analysis and Computer Programs show that it is practical to truncate the waveform at a point where the amplitude of the oscillations has reached 86 per cent of the final value. This conclusion makes the requirements for waveform resolution easier to meet and, except for transducers with very little damping, makes the CRT representation adequate for determining the transfer function.

DRIFT The problem of drift in the system calibration could not be solved by minor modification of the equipment. To minimize drift the equipment should be allowed to warm up for an hour before photographing the transient and two hours before digitizing the waveform. Solution of this problem requires a major modification of the calibration facility. The proposed modification is described in the next section. In addition it is recommended that for maximum accuracy the X axis beam positioning voltage be derived from a laboratory type 0.01% regulated power supply. This will require that the proper terminal be made available on the front panel.

CONCLUSIONS AND RECOMMENDATIONS

The system is now fully operable but, due to drift in the calibration of the electronic equipment, does not provide for maximum accuracy of the data produced. Drift has been found to cause errors as high as 20%, discounting the possibility that calibration adjustments might be changed inadvertently.

With the addition of a calibration waveform the present FSADC system is satisfactory for obtaining and digitizing transient waveforms. This conclusion is based on the results of the mathematical analysis which verify that an accurate transfer function can be obtained from truncated data.

To achieve maximum accuracy with the present FSADC system, the system should be calibrated after a two hour warm-up period and immediately before the recording or digitizing operation. Since most sources of error are common, they would tend to cancel when both transient and calibrating waveforms are entered on the same transparency. The sources of error include oscilloscope vertical amplifier long-term drift, optical errors, oscilloscope vertical sweep linearity, and errors due to placement of the transparency holder in the Flying Spot Scanner. If a known calibration waveform is inserted on each transient

waveform transparency recorded by the FSADC, then the need for frequent equipment calibration and extended warm-up periods will no longer exist. System operational procedures will also be simplified, and accuracy will be improved. Advantages are as follows: (1) All required information would be contained on a single transparency, Figure 29. (2) Digitizing of the calibrating information and the transient would be done in the same operation. The computer program would compute the transient digital data using the calibration information. (3) The added feature of an adjustable time scale would permit recording a maximum amount of data. This is not possible at present because the sweep time must be changed in relatively large steps. (4) A continuously variable vertical adjustment could be used as calibration information is contained in the transparency.

It is strongly recommended that a Calibration Waveform Generator be incorporated into the FSADC system. An earlier recommendation that a magnetic data recording system be developed, is withdrawn. Since data truncation proved feasible, there is no strong justification for investment required to develop a high frequency recording system.

TABLE I TRANSFER FUNCTION AMPLITUDE AND PHASE CHARACTERISTICS COMPUTED NEAR NATURAL FREQUENCIES AS A FUNCTION OF INPUT DATA TRUNCATION

FREQUENCY	INPUT DATA SET				
	ONE	TWO	THREE	FOUR	KNOWN
CPS	TIME CONSTANT	TIME CONSTANTS	TIME CONSTANTS	TIME CONSTANTS	TRANSFER FUNCTION
2051	13.83 $\angle -43.1^\circ$	12.23 $\angle -34.7^\circ$	12.25 $\angle -36.8^\circ$	12.28 $\angle -36.7^\circ$	12.21 $\angle -36.8^\circ$
*2151	17.12 $\angle -90.8^\circ$	20.01 $\angle -91.0^\circ$	20.66 $\angle -90.8^\circ$	20.65 $\angle -91.1^\circ$	20.68 $\angle -90.8^\circ$
2251	14.07 $\angle -115.1^\circ$	12.58 $\angle -145.5^\circ$	12.55 $\angle -143.6^\circ$	12.46 $\angle -143.7^\circ$	12.50 $\angle -143.9^\circ$
3701	10.83 $\angle -222.8^\circ$	10.74 $\angle -203.8^\circ$	9.43 $\angle -204.9^\circ$	9.72 $\angle -207.9^\circ$	9.77 $\angle -206.6^\circ$
*3776	11.75 $\angle -263.9^\circ$	15.73 $\angle -264.5^\circ$	17.06 $\angle -264.5^\circ$	17.58 $\angle -264.4^\circ$	17.70 $\angle -264.5^\circ$
3851	9.88 $\angle -306.3^\circ$	9.67 $\angle -326.5^\circ$	8.63 $\angle -326.3^\circ$	8.70 $\angle -324.5^\circ$	8.73 $\angle -324.4^\circ$

* Natural frequency for system

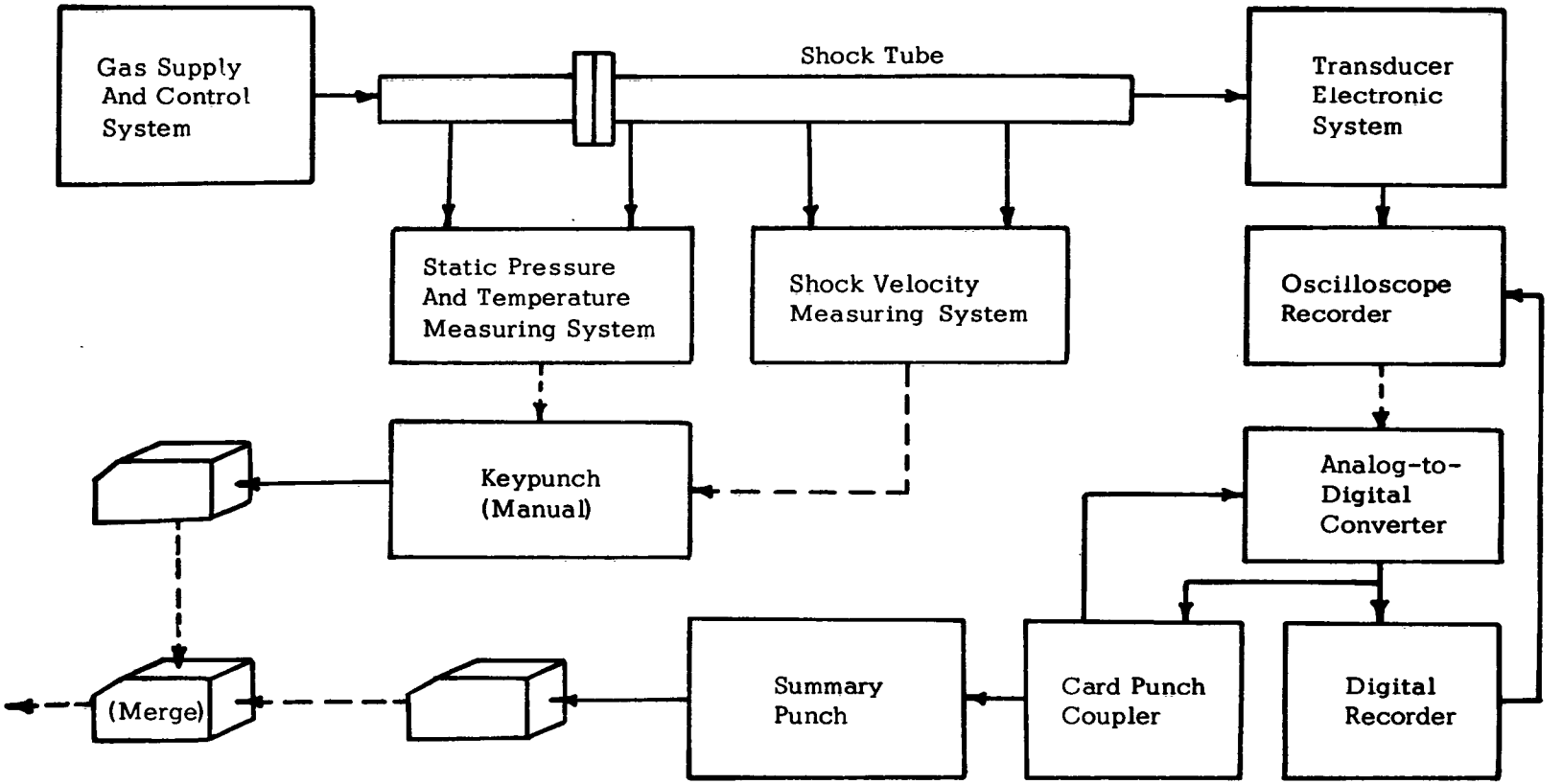

FIGURE 1 EDWARDS AFB SHOCK-TUBE FACILITY SCHEMATIC

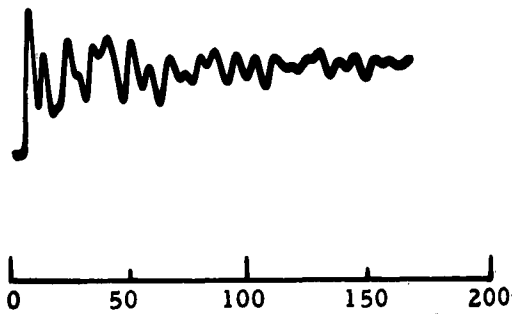

(a) Transducer Response to Input Step

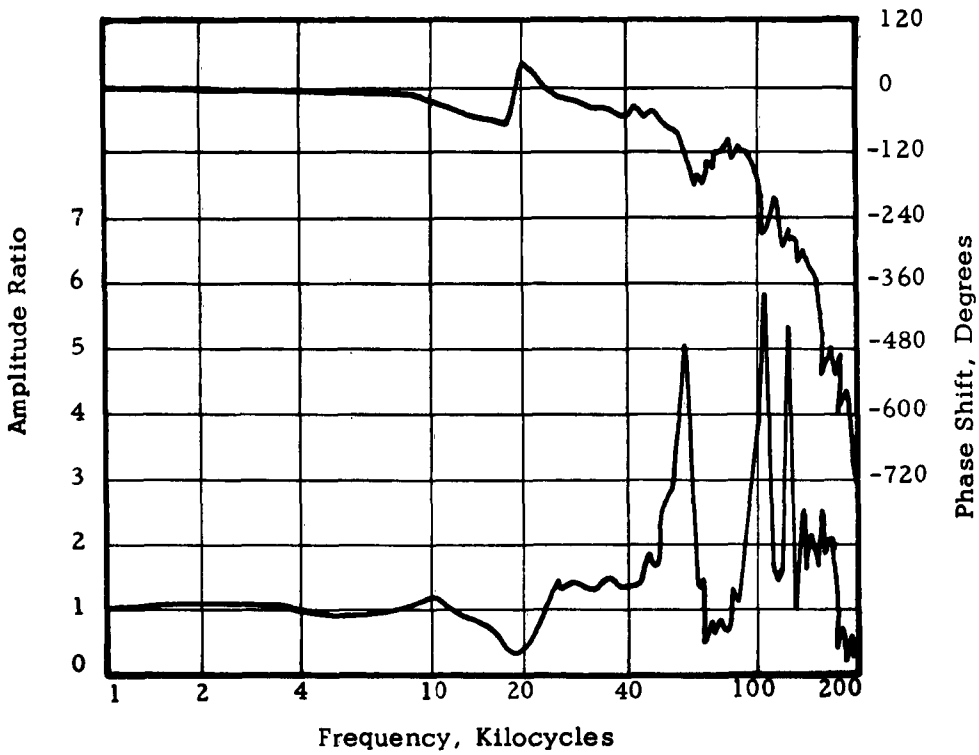

(b) Computed Transducer Frequency Response

FIGURE 2 SYSTEM TRANSFER FUNCTION FOR ELASTRONICS TRANSDUCER MODEL PB-2K

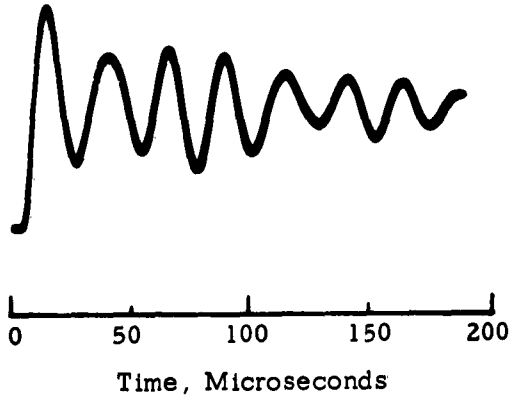

(a) Transducer Response to Input Step

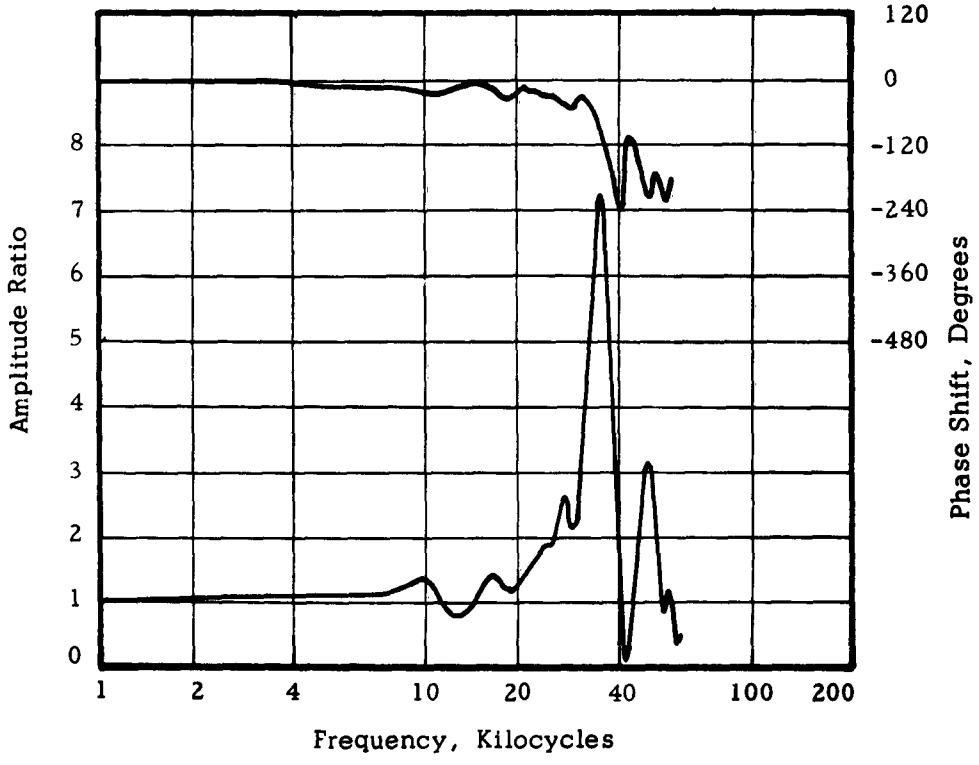

(b) Computed Transducer Frequency Response

FIGURE 3 SYSTEM TRANSFER FUNCTION FOR KISTLER PZ14 TRANSDUCER

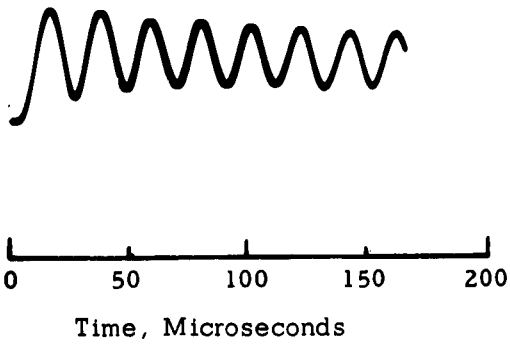

(a) Transducer Response to Input Step

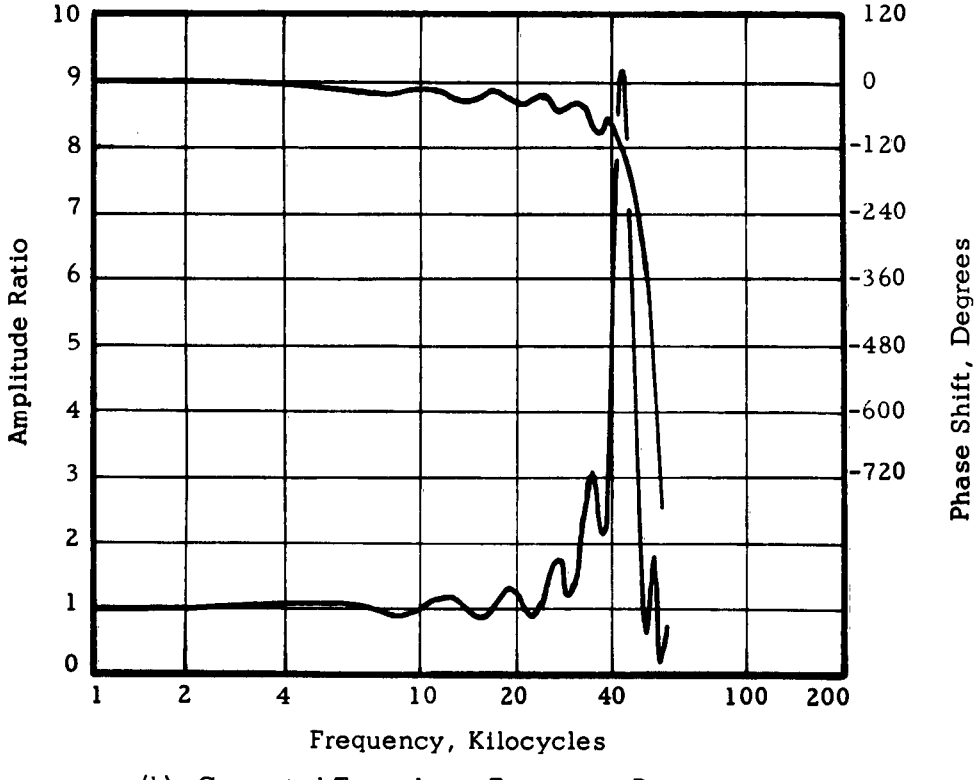

(b) Computed Transducer Frequency Response

FIGURE 4 SYSTEM TRANSFER FUNCTION FOR NORWOOD MODEL 101

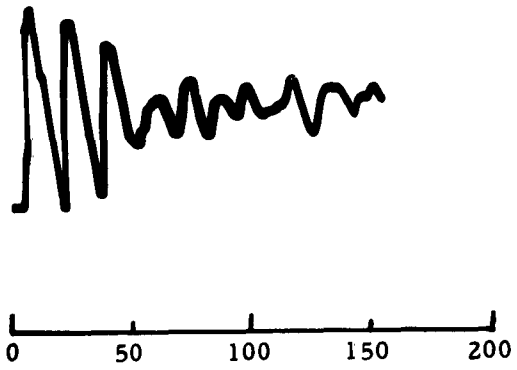

(a) Transducer Response to Input Step

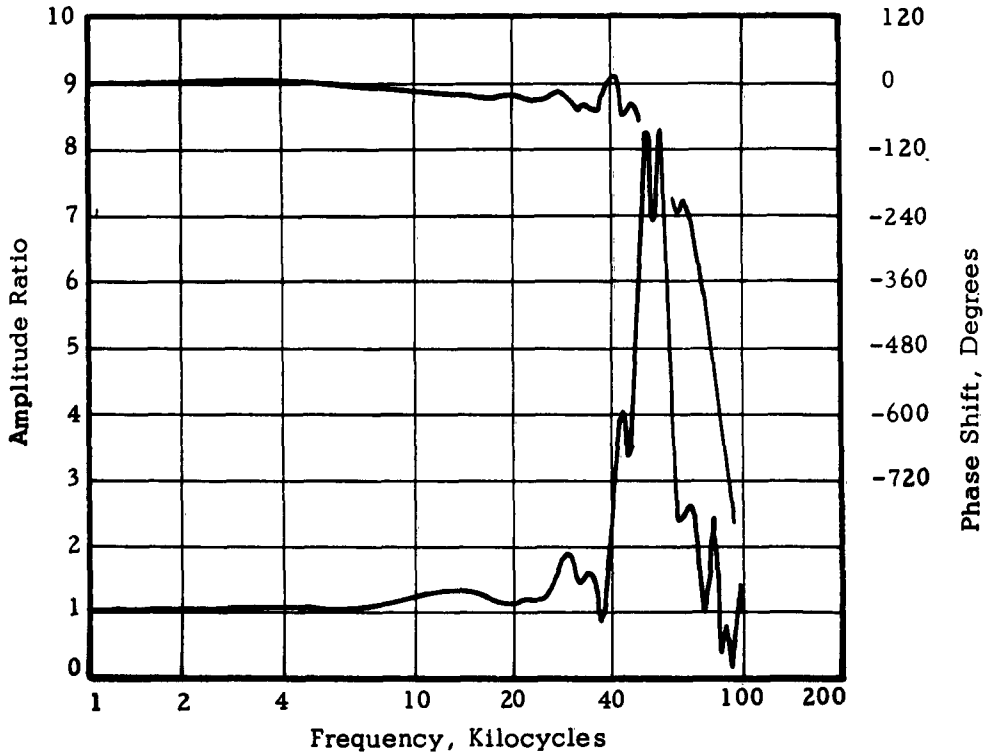

(b) Computed Transducer Frequency Response

FIGURE 5 SYSTEM TRANSFER FUNCTION FOR ENDEVCO MODEL 2502

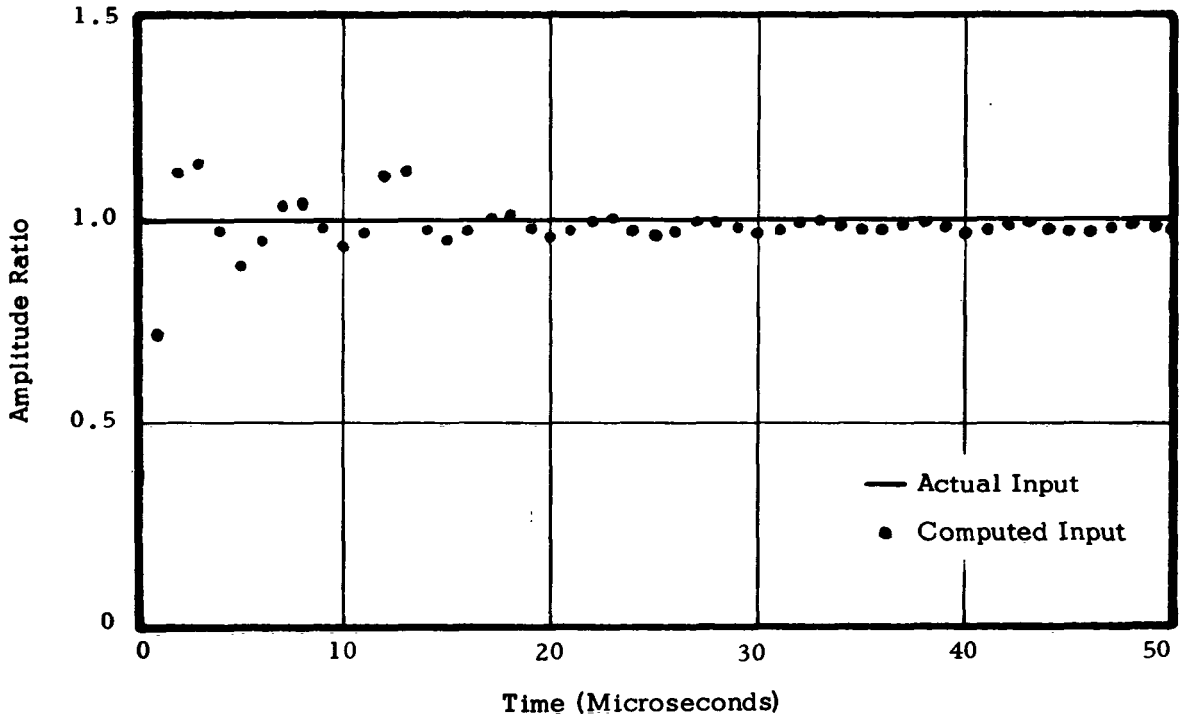

FIGURE 6 INPUT STEP COMPUTED FROM ELASTRONICS MODEL PB-2K TIME RESPONSE AND INVERSE TRANSFER FUNCTION

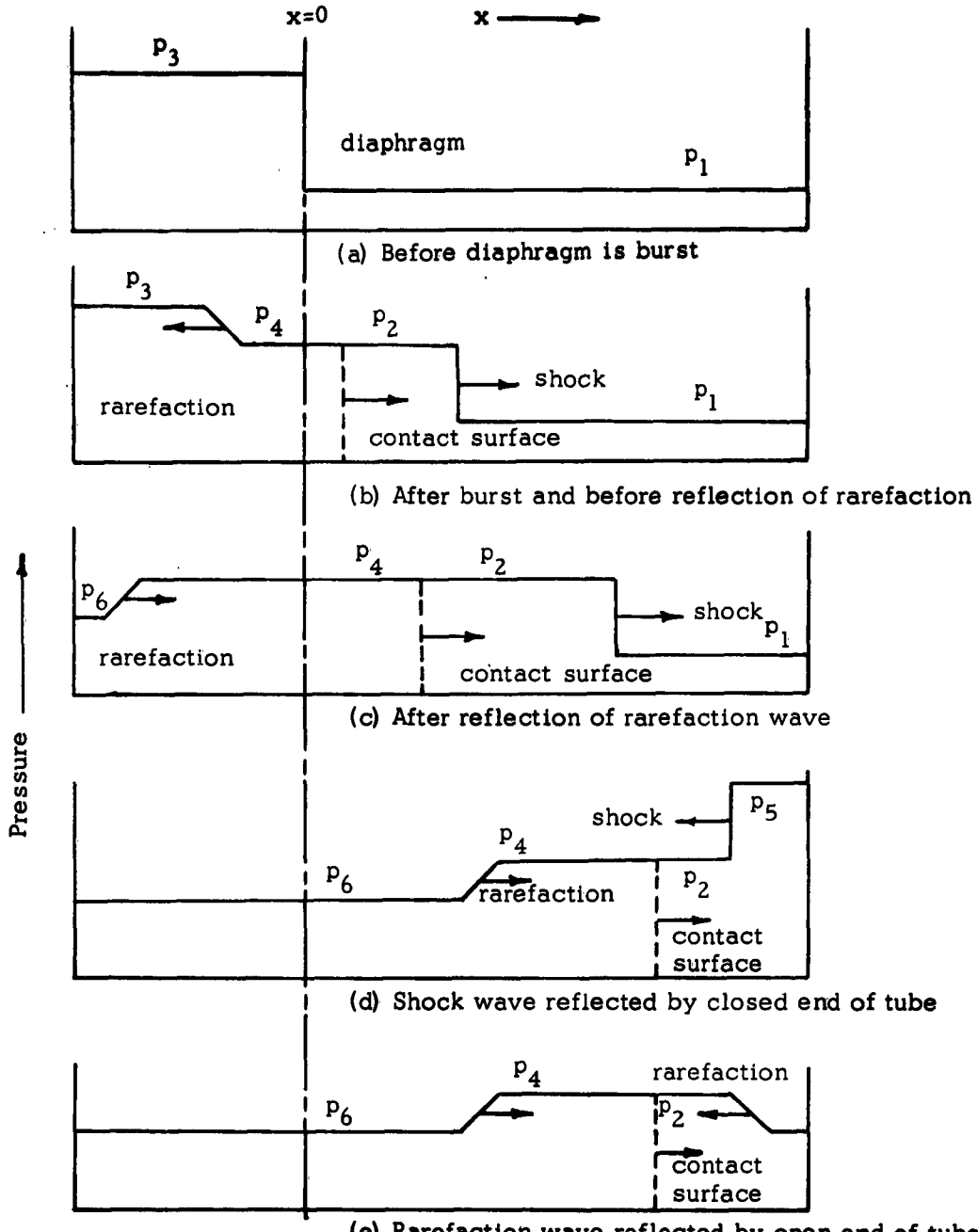

FIGURE 7 PRESSURES AND WAVES IN SHOCK TUBE

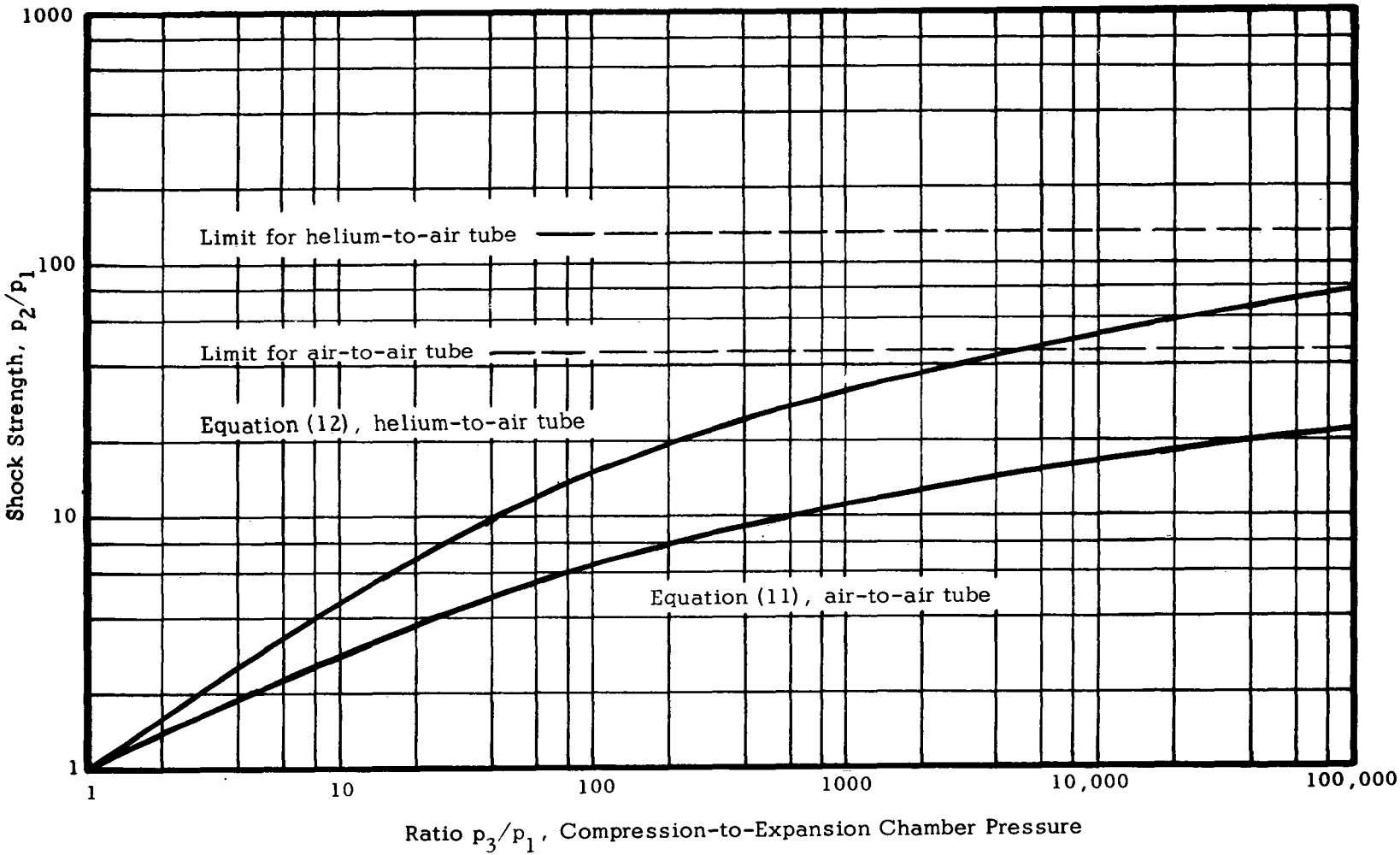

FIGURE 8 RELATION BETWEEN COMPRESSION CHAMBER PRESSURE AND SHOCK STRENGTH

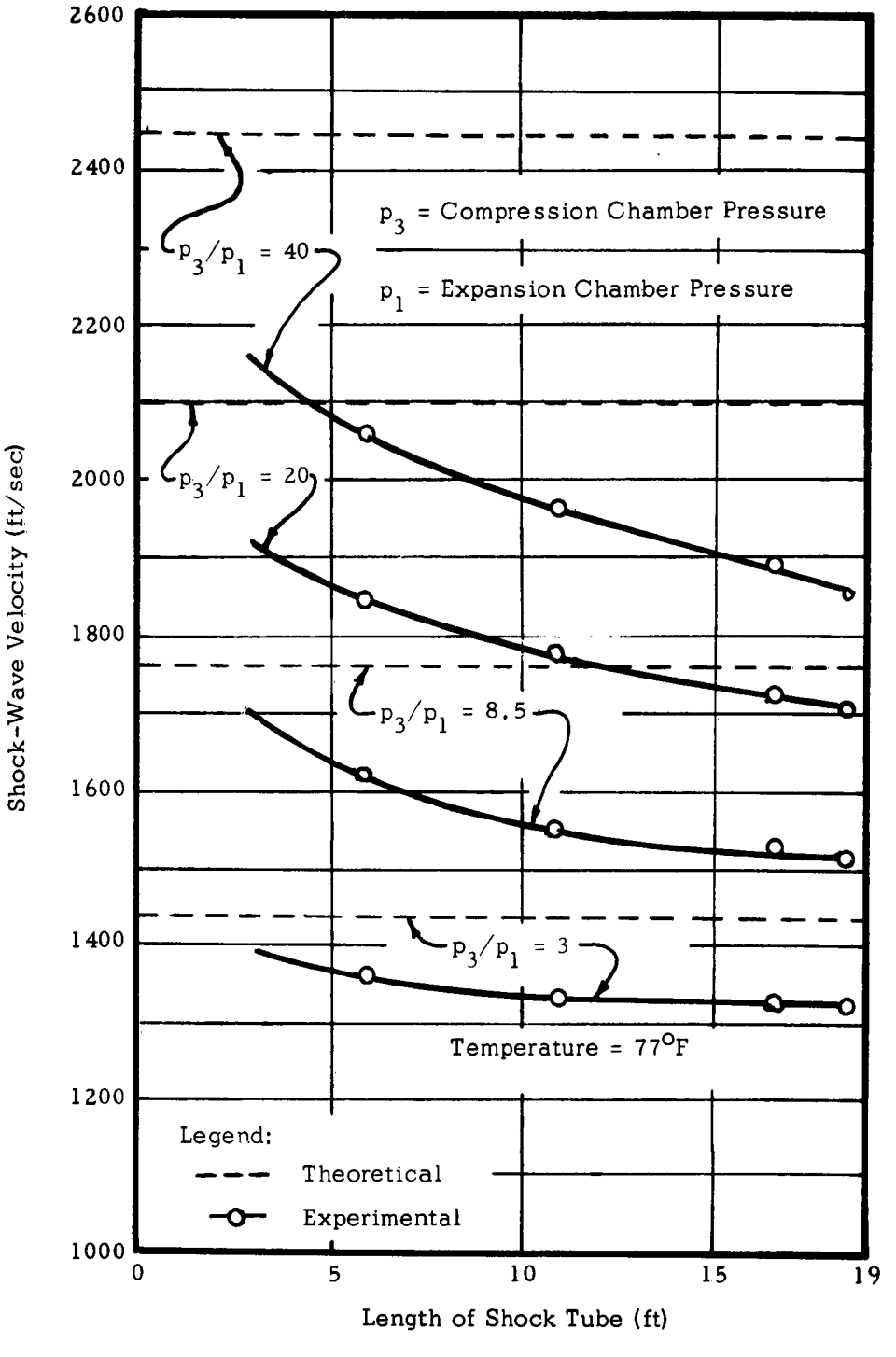

FIGURE 9 SHOCK-WAVE VELOCITY ATTENUATION

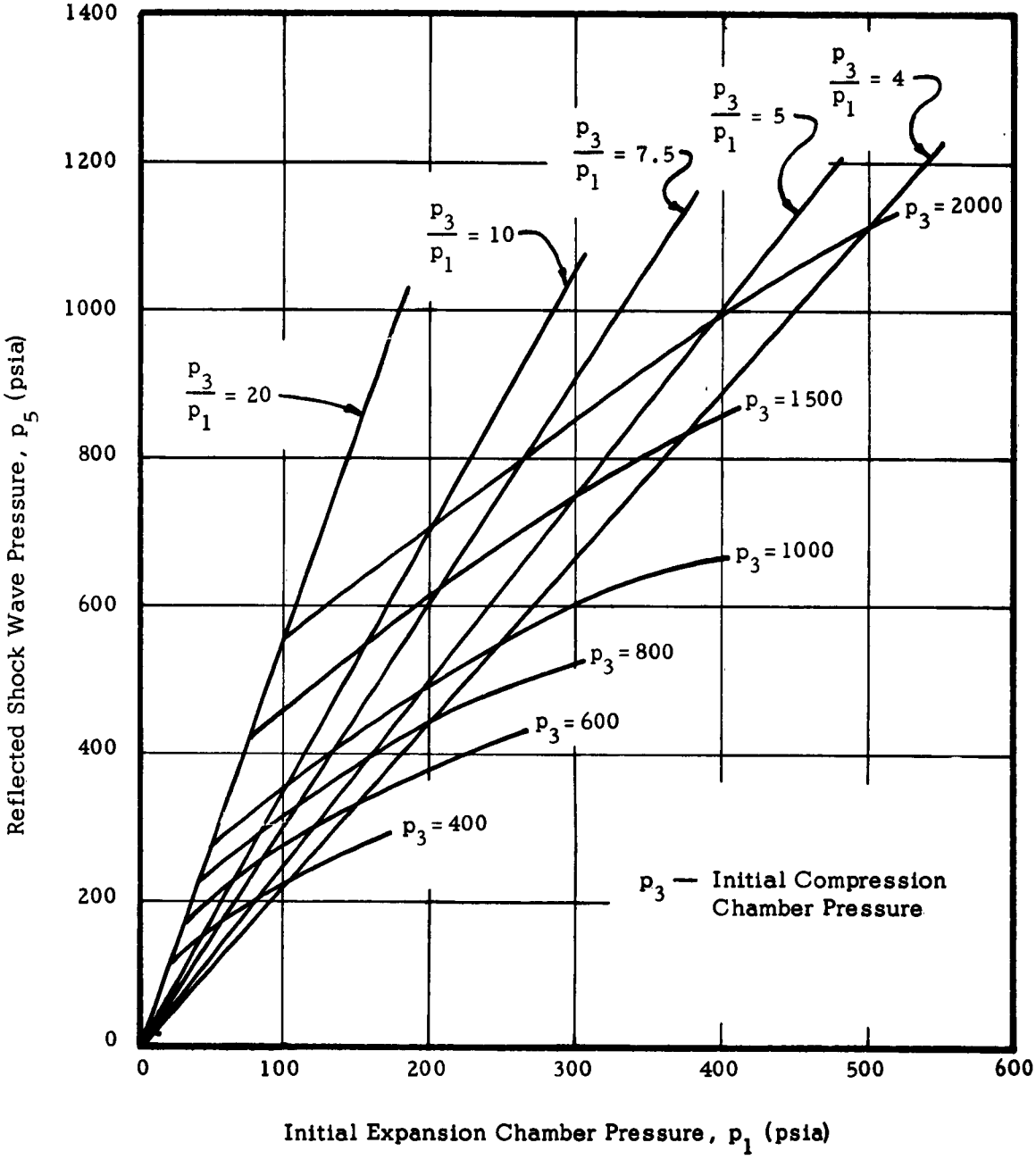

FIGURE 10 SHOCK TUBE CALIBRATION CURVE

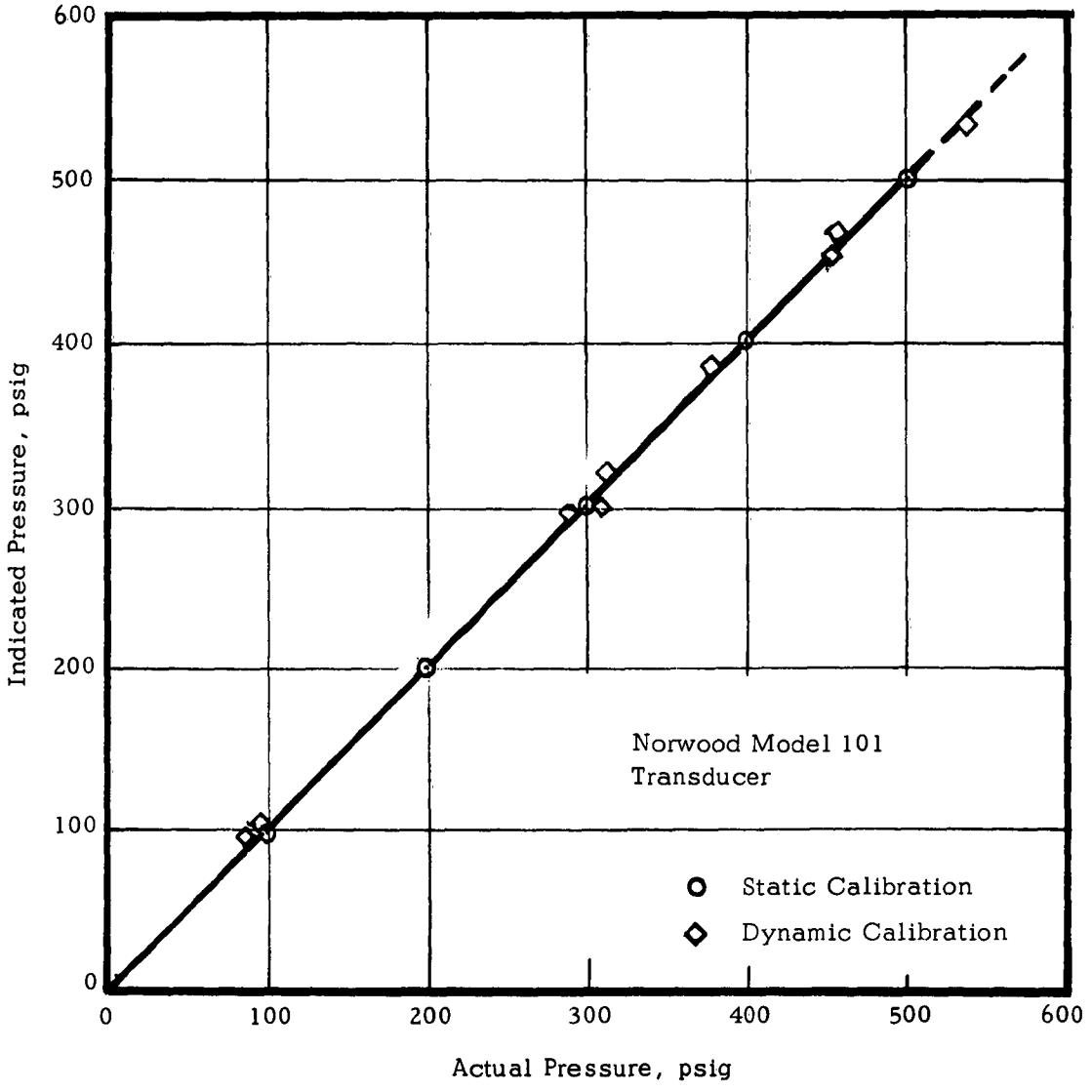

FIGURE 11 CALIBRATION CURVE FOR NORWOOD MODEL 101 TRANSDUCER

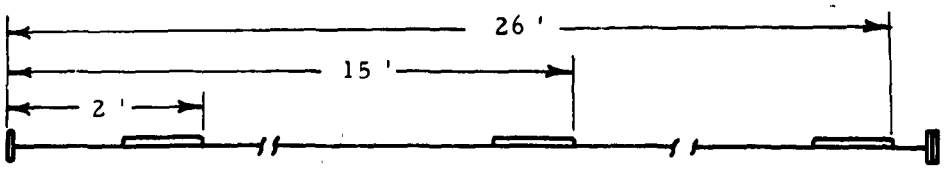

NOTE: Distances are measured from the open end of the shock tube to the bulb end of the thermometers.

LOCATION OF THERMOMETERS ON SHOCK TUBE

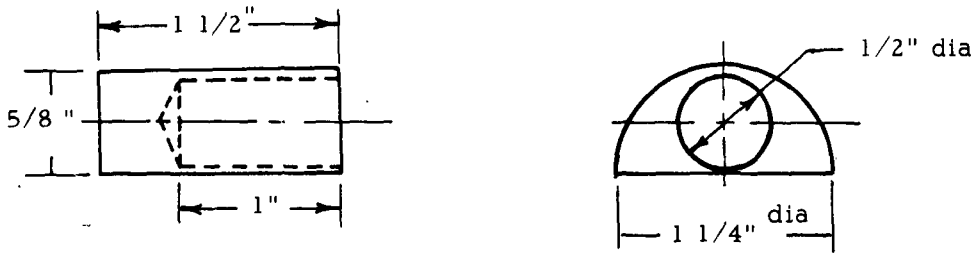

NOTES: Construct from aluminum barstock
Two required for each assembly
Fasten to shock tube with automobile radiator-hose straps

HOLDER DETAILS

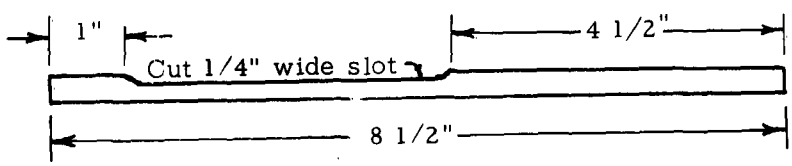

NOTE: Construct from 1/2" OD, 1/16" wall aluminum tubing

PROTECTION TUBE DETAILS

THERMOMETER SPECIFICATIONS

Mercury-in-Glass
8 1/4" long, 1/4" dia
54° — 101° Range, 1/2° divisions

FIGURE 12 THERMOMETER INSTALLATION DETAILS

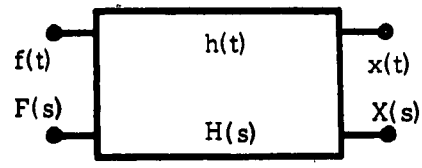

FIGURE 13 TYPICAL TRANSDUCER SYSTEM

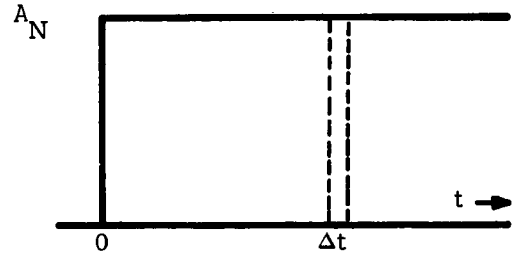

FIGURE 14 TYPICAL STEP FUNCTION

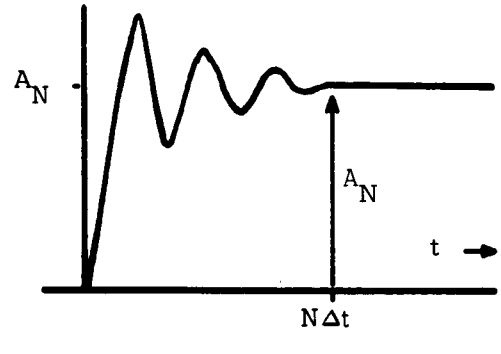

FIGURE 15 TYPICAL OUTPUT FOR STEP INPUT

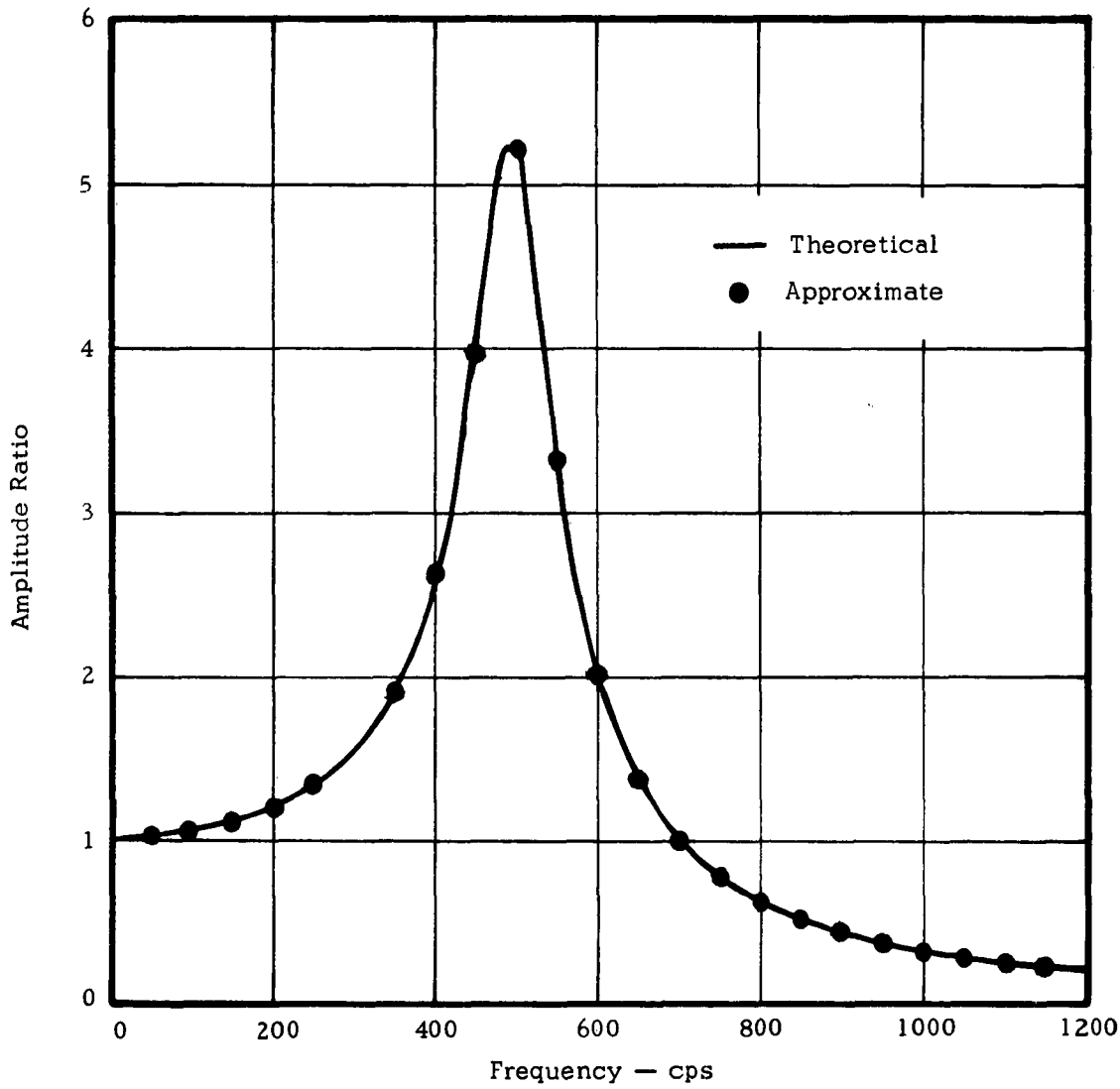

FIGURE 16 AMPLITUDE CHARACTERISTICS OF THE TRANSFER FUNCTION FOR A SINGLE-DEGREE-OF-FREEDOM SYSTEM

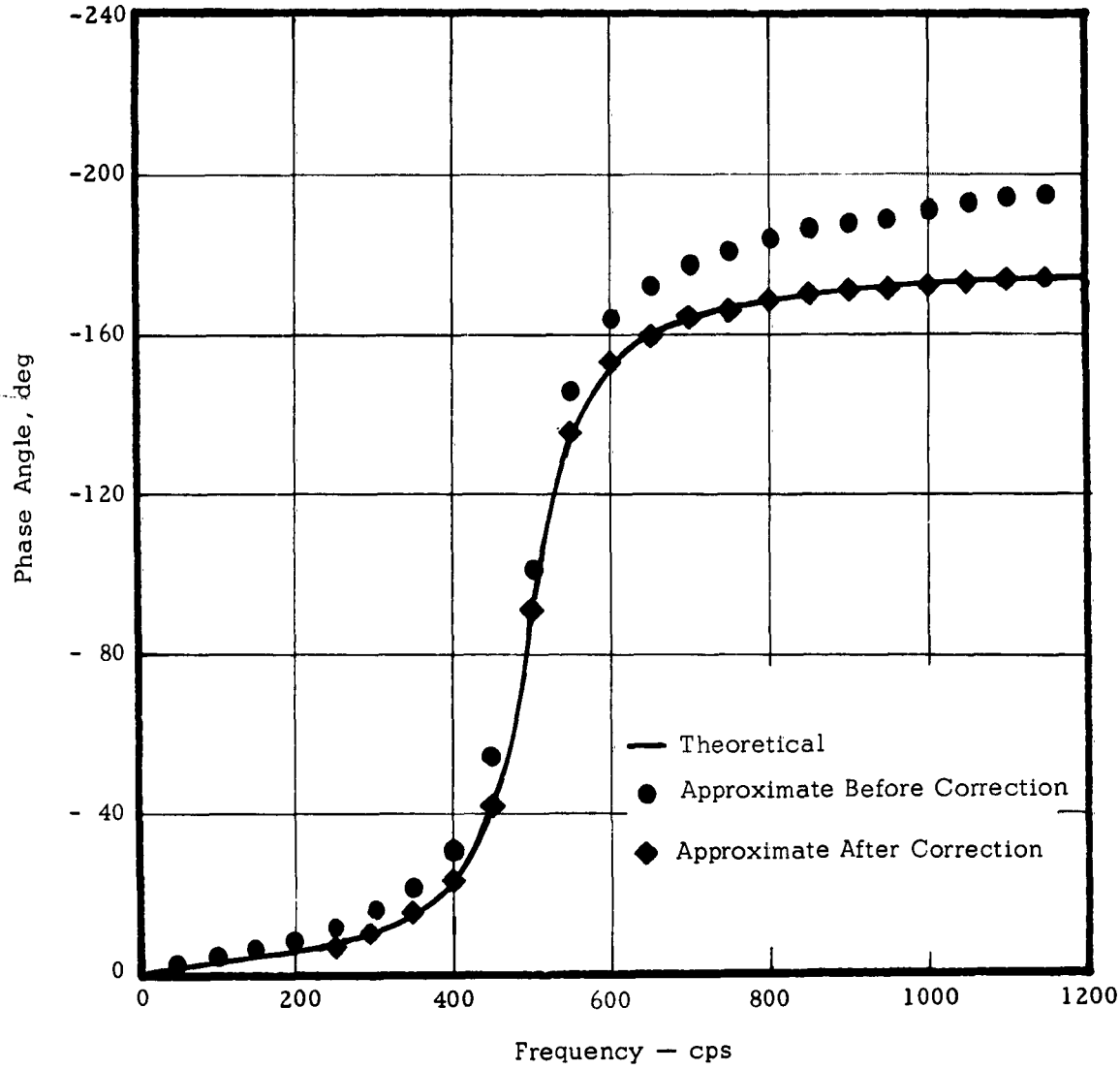

FIGURE 17 PHASE CHARACTERISTICS OF THE TRANSFER FUNCTION FOR A SINGLE-DEGREE-OF-FREEDOM SYSTEM

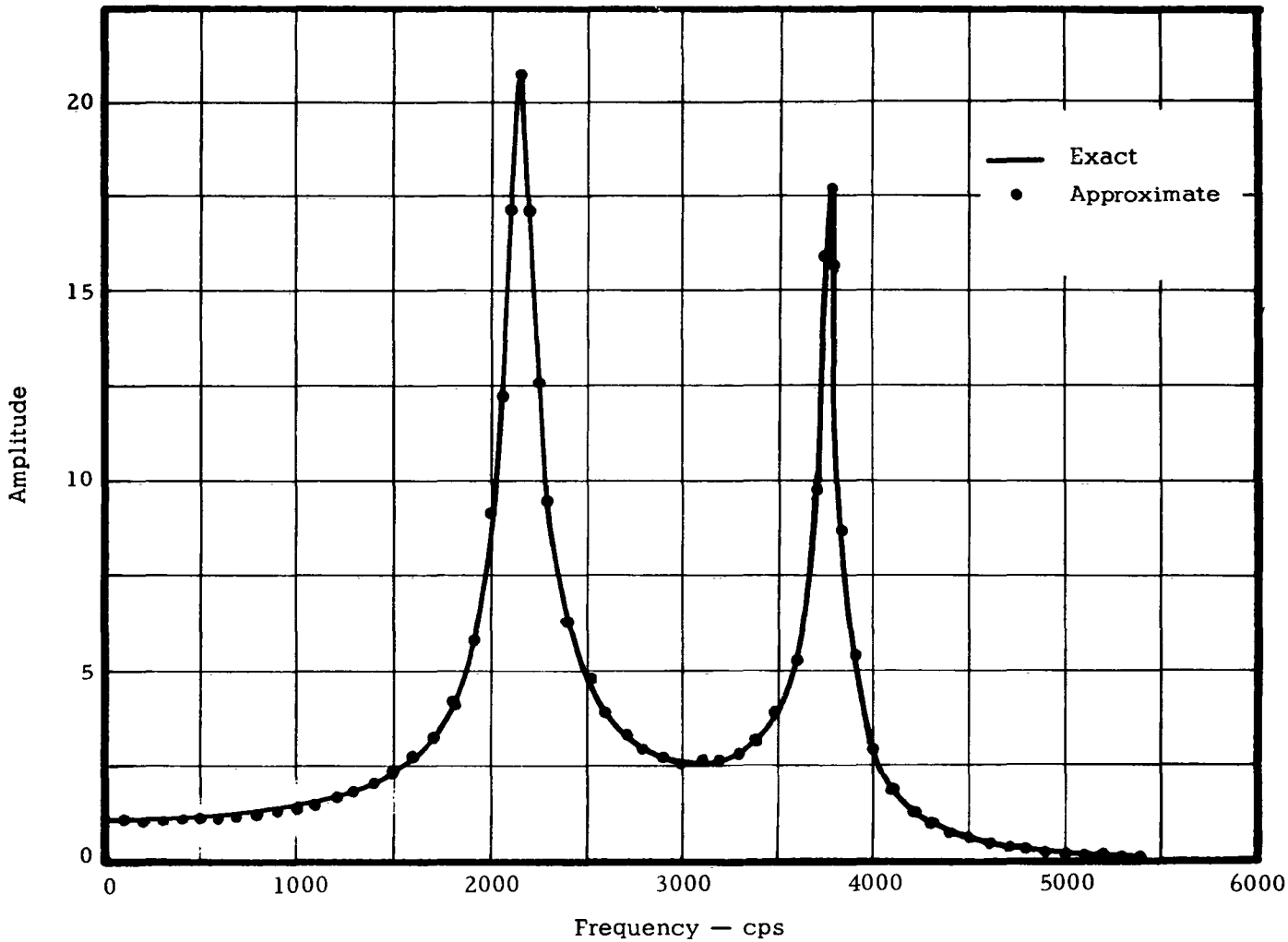

FIGURE 18 AMPLITUDE CHARACTERISTIC VS FREQUENCY
TWO-DEGREES-OF-FREEDOM SYSTEM TRANSFER FUNCTION

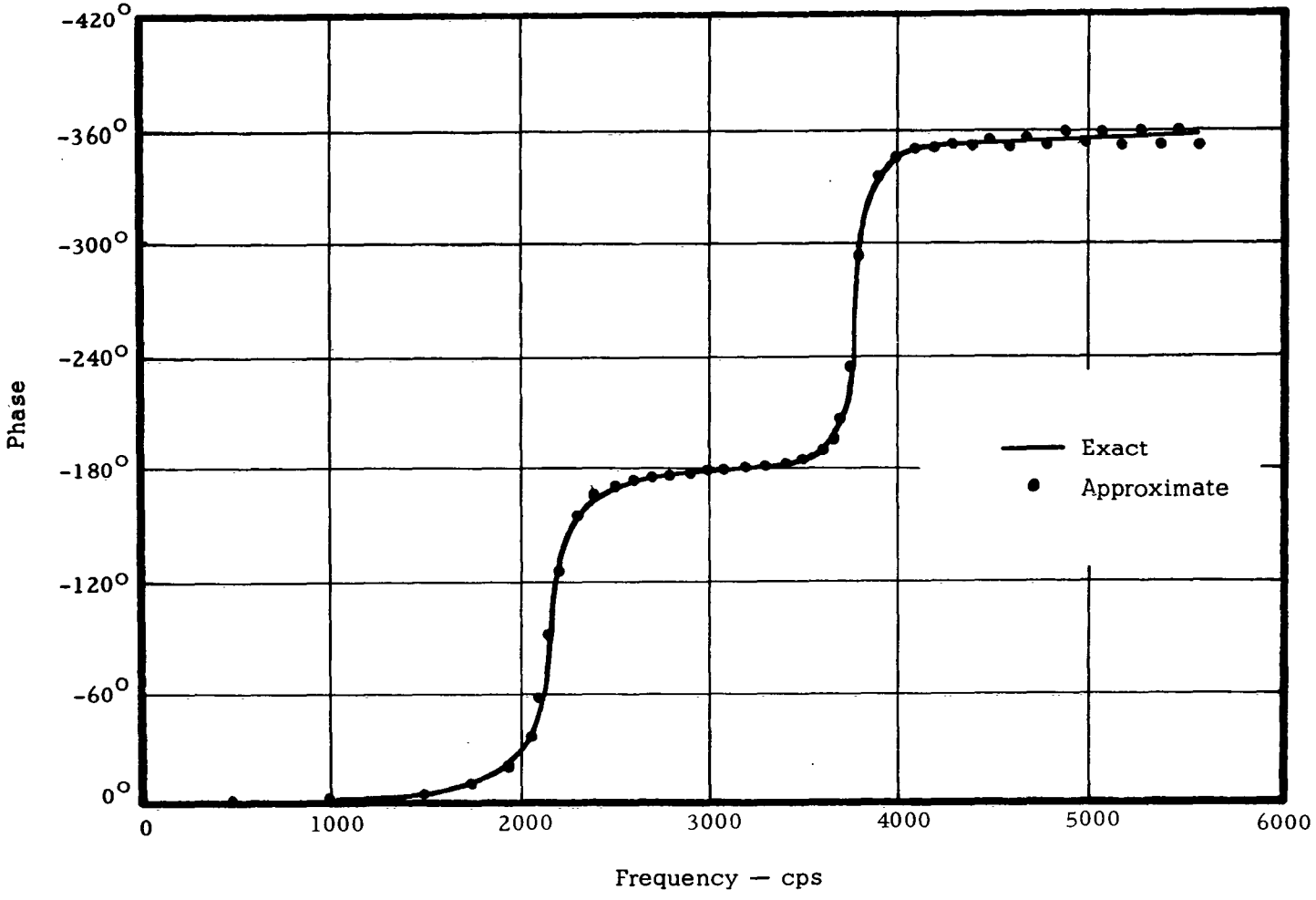

FIGURE 19 PHASE CHARACTERISTIC VS FREQUENCY
TWO-DEGREES-OF-FREEDOM SYSTEM TRANSFER FUNCTION

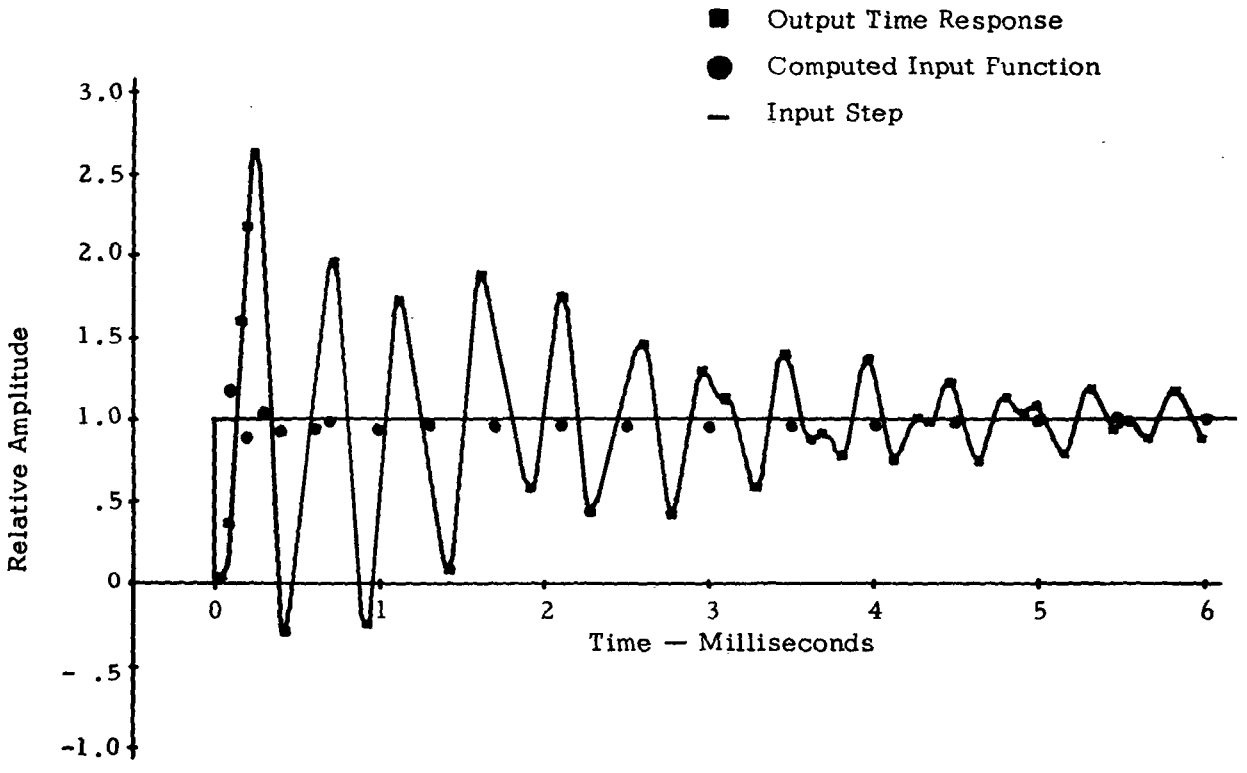

FIGURE 20 OUTPUT RESPONSE VS TIME
(Two Degree of Freedom System)

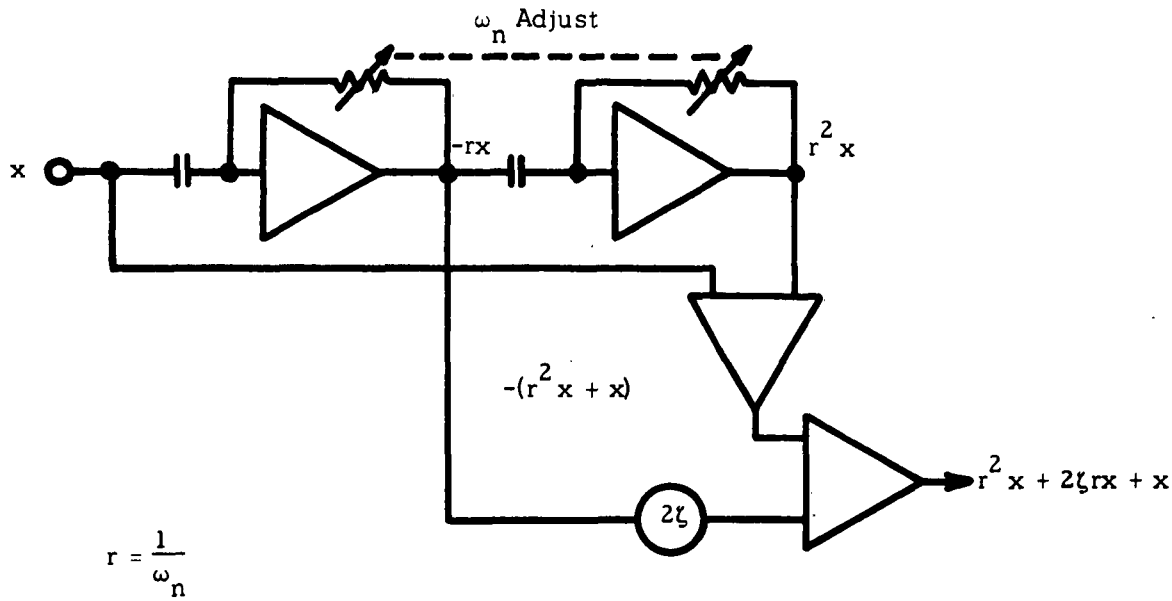

FIGURE 21 ANALOG COMPUTER INVERSE TRANSFORM REALIZATION

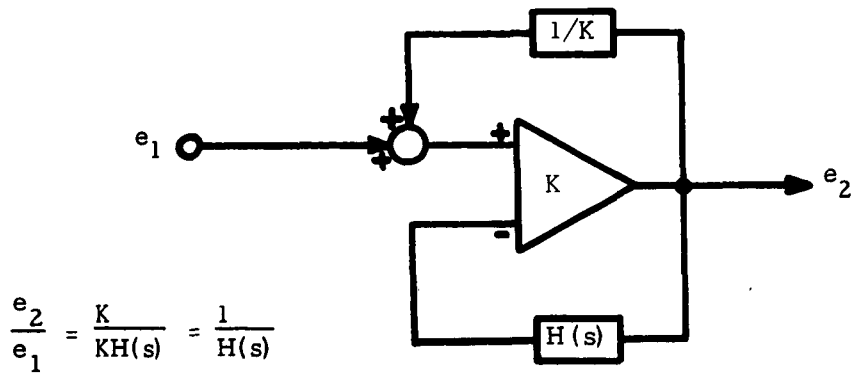

FIGURE 22 EXACT INVERSE TRANSFER FUNCTION REALIZATION

(Chart speed 25 millimeters per second)

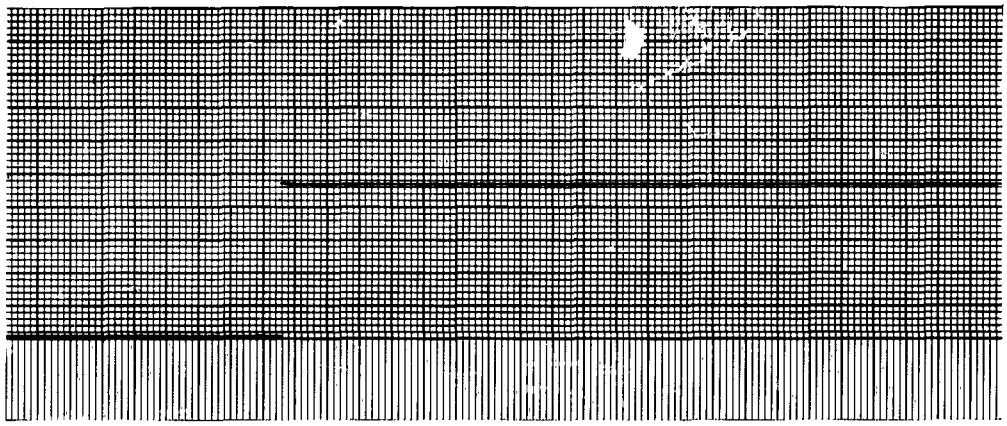

(a) Recorded Step Input

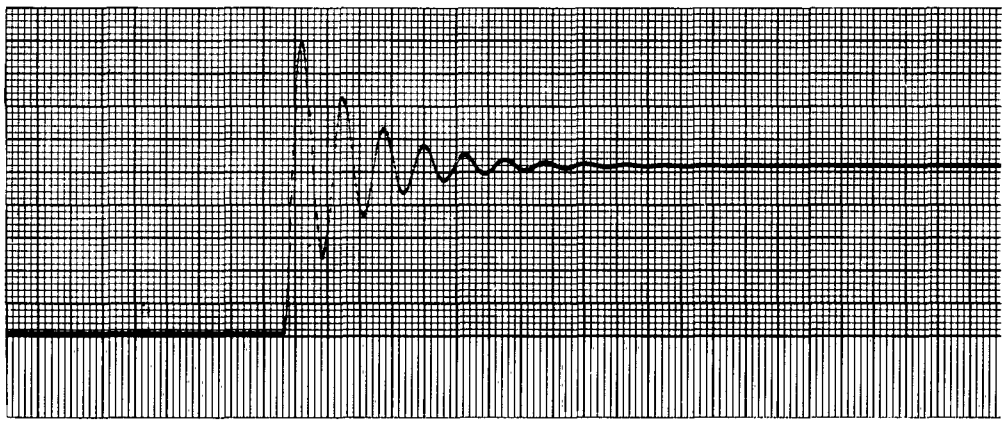

(b) Time Response

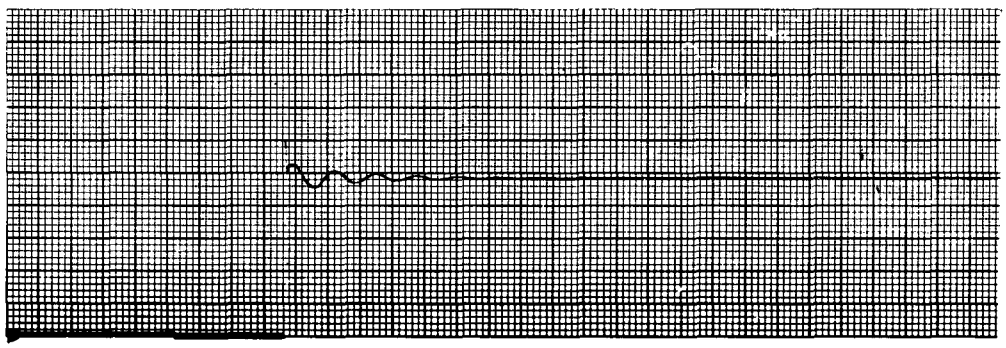

(c) Compensated Time Response

FIGURE 23 ANALOG COMPENSATION OF OUTPUT RESPONSE

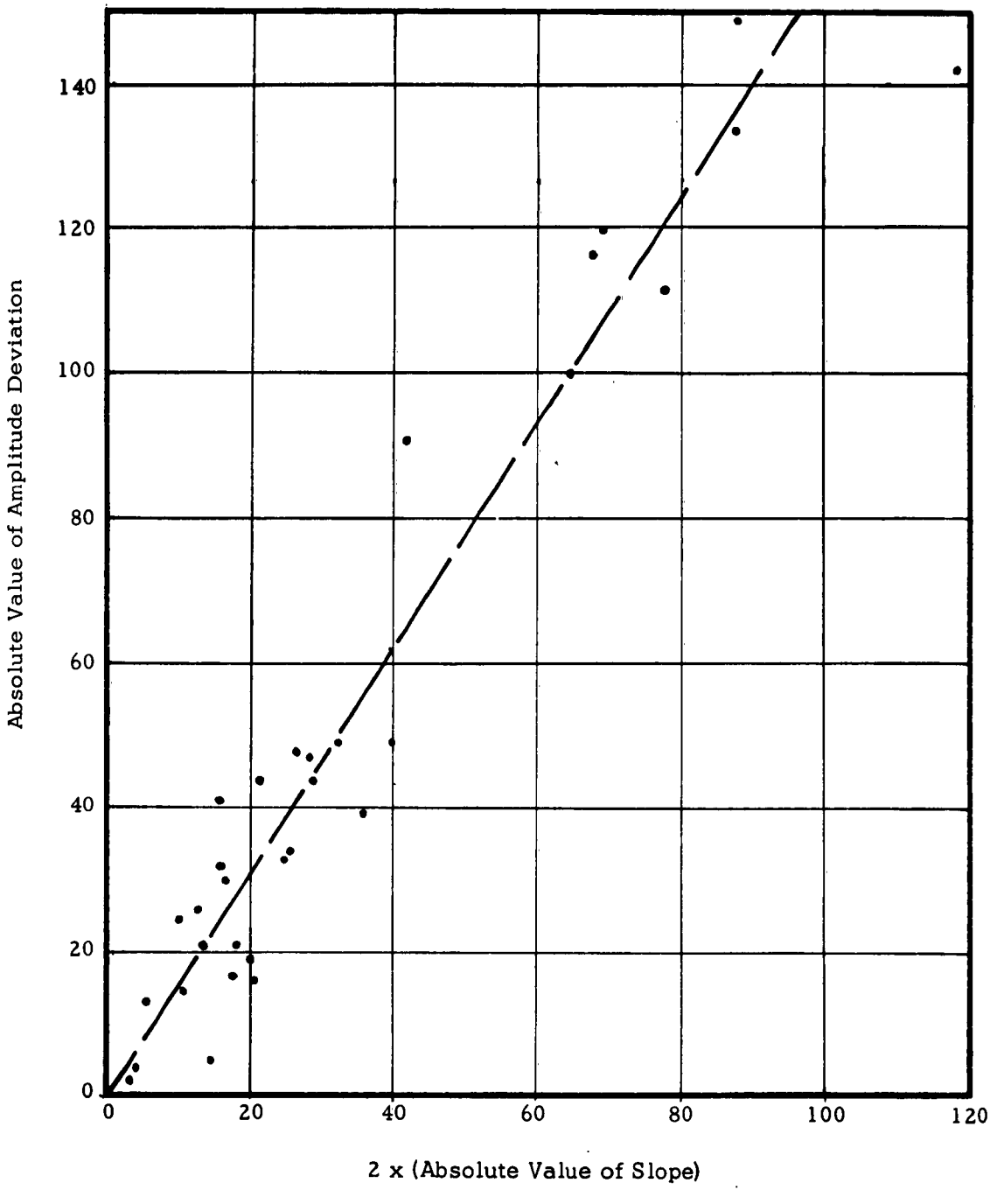

FIGURE 24 SHORT TERM ERROR ANALYSIS

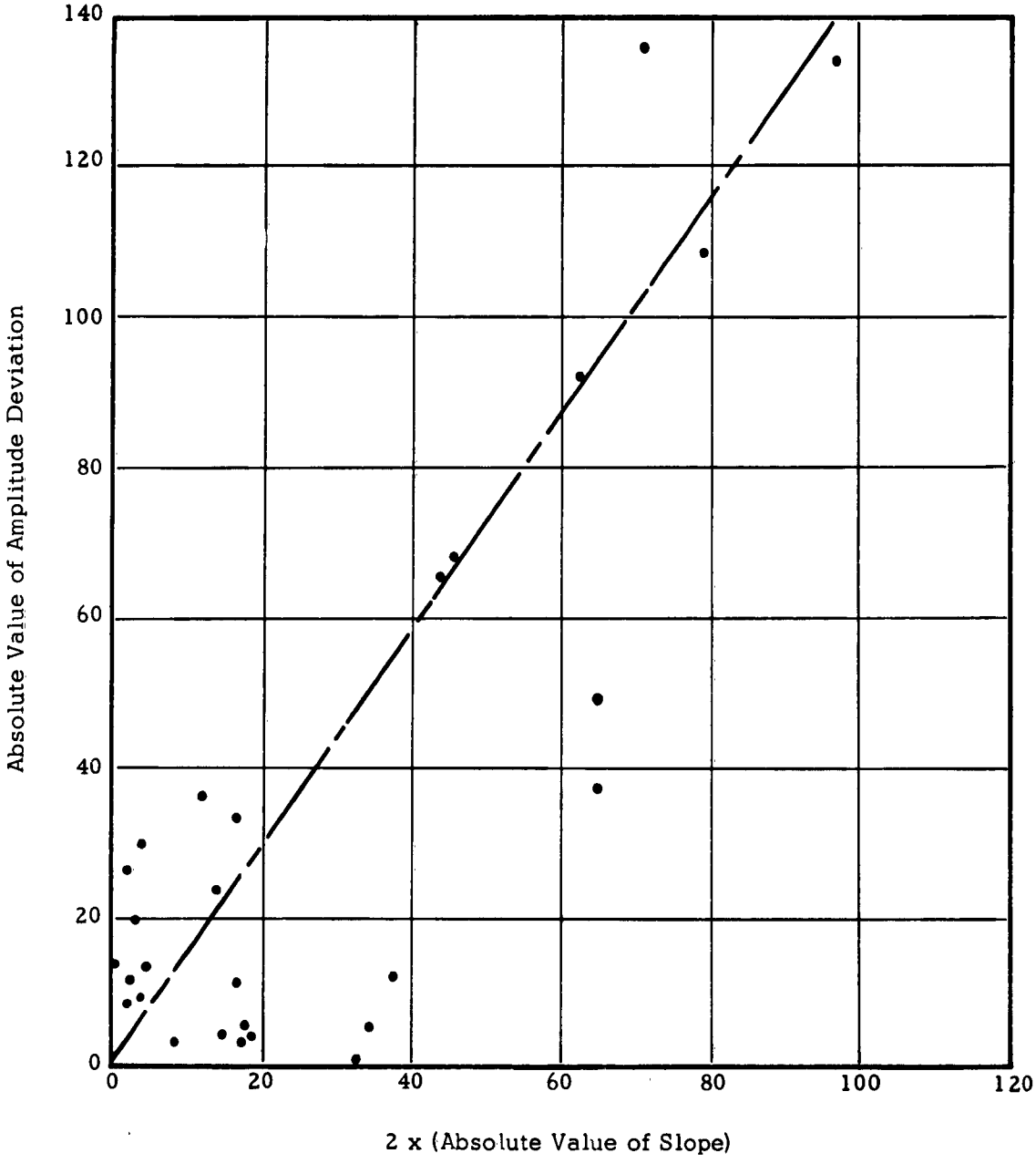

FIGURE 25 LONG TERM ERROR ANALYSIS

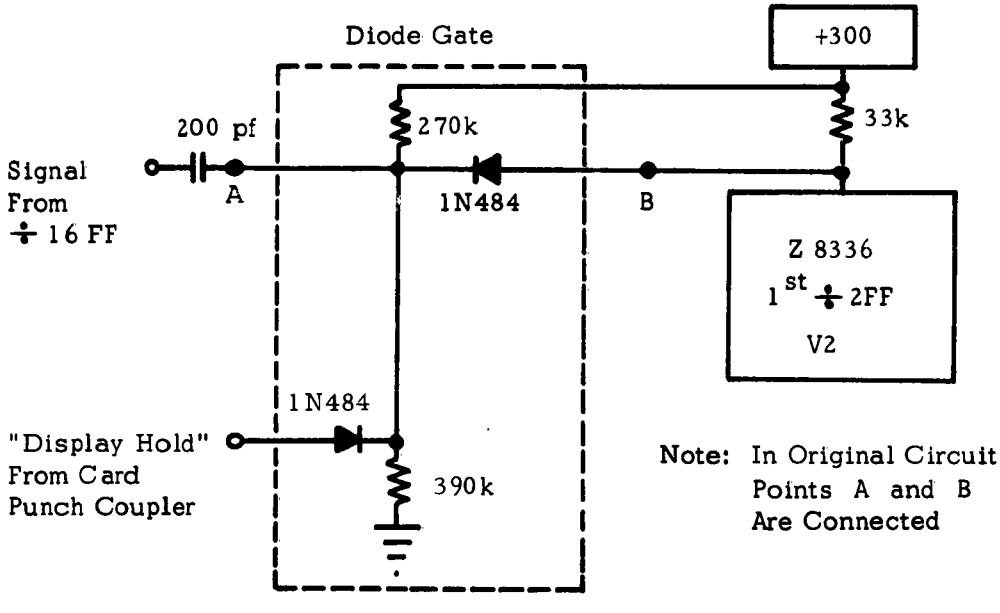

FIGURE 26 SYNCHRONIZING GATE

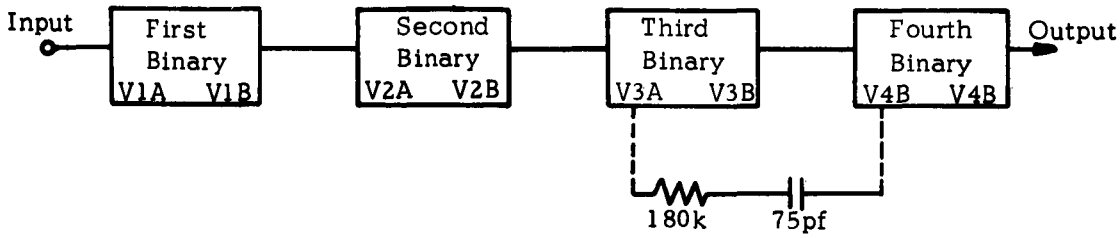

Conversion of X16 to X12 Scaler

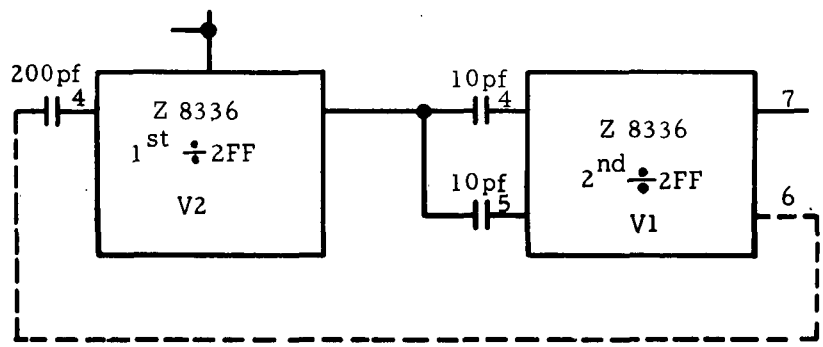

Conversion of X4 to X3 Scaler

FIGURE 27 CONVERSION OF SCALERS

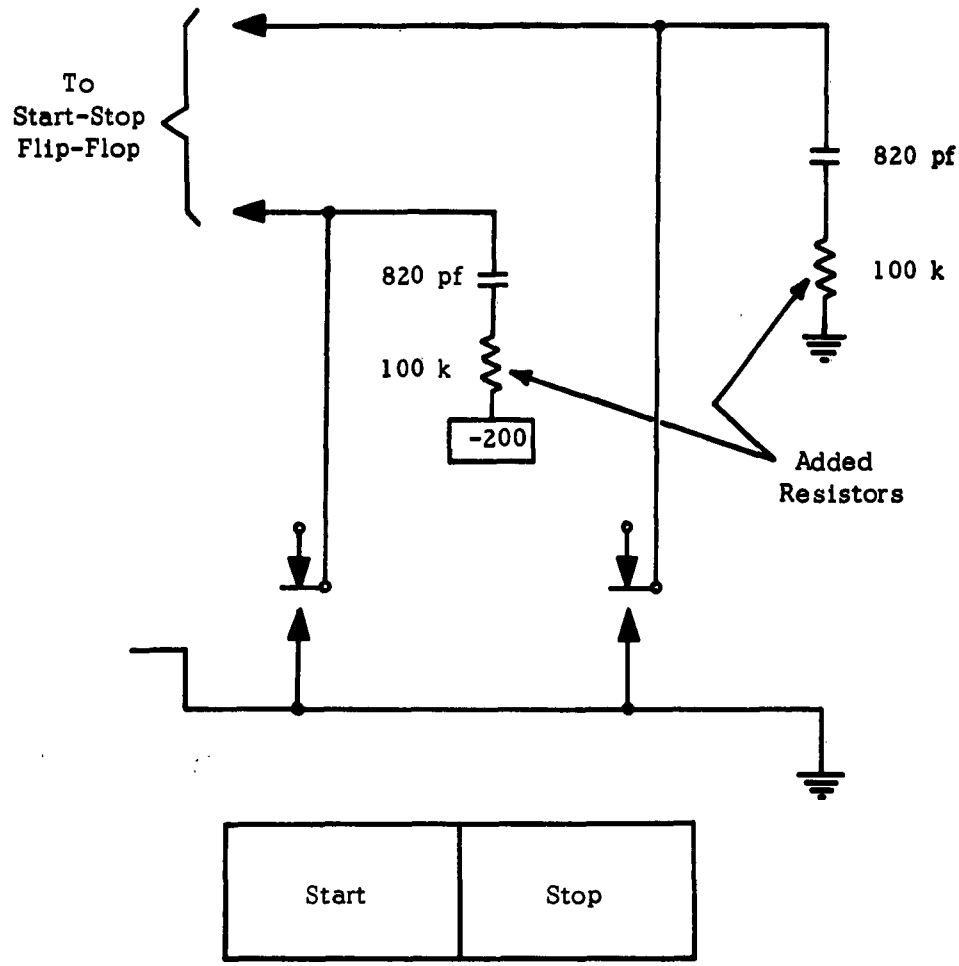

FIGURE 28 MODIFICATION TO ELIMINATE ERRATIC COUNTER OPERATION

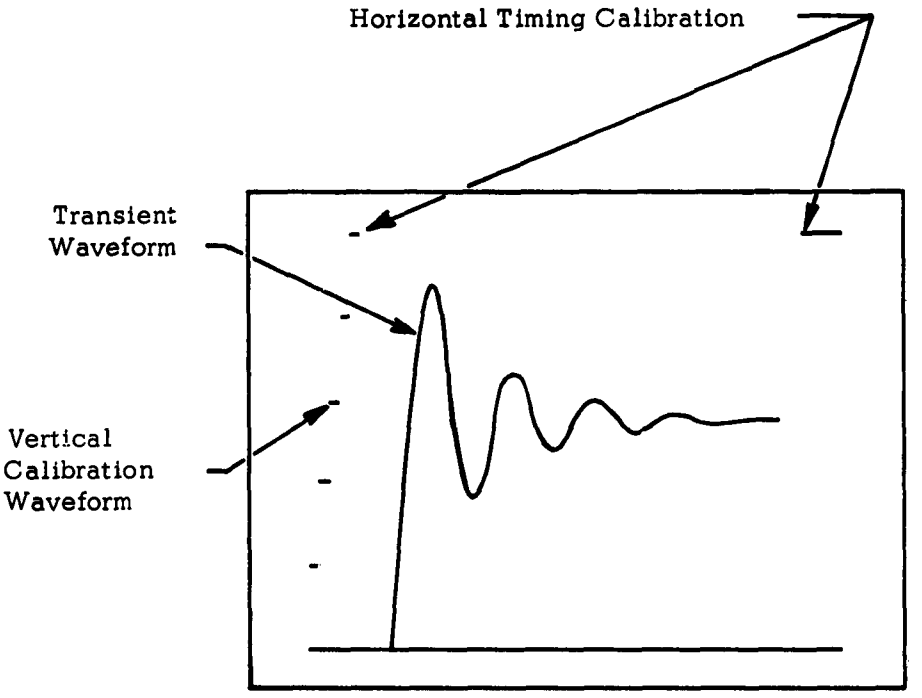

FIGURE 29 TRANSPARENCY WITH CALIBRATION DATA

REFERENCES

(1) R B Bowersox and J Carlson, "Digital-Computer Calculation of Transducer Frequency Response From Its Response to a Step Function", Progress Report No 20-311 (Contract No DA-04-495-Ord18), Jet Propulsion Laboratory, (26 July 1957).

(2) G R Cowan and D F Hornig, "The Experimental Determination of the Thickness of a Shock Front in a Gas", J Chem Phys 18, p 1,008-18 (August 1950).

(3) A H Shapiro, "The Dynamics and Thermodynamics of Compressible Fluid Flow", Volume II, The Ronald Press Company, New York, 1954.

(4) J K Wright, "Shock Tubes", John Wiley & Sons, Inc, New York, 1961.

(5) A E Wolfe, "Shock Tube for Gage Performance Studies", Report No 20-87 (Contract No DA-04-495-Ord18), Jet Propulsion Laboratory, (May 1955).

(6) R L Trimpi and N B Cohen, "A Theory for Predicting the Flow of Real Gases in Shock Tubes with Experimental Verification", NACA Technical Note 3375, (1955).

(7) Mischa Schwartz, "Information Transmission, Modulation, and Noise", p 169-172, McGraw-Hill Book Company, Inc, New York, 1959.

(8) R W Hamming, "Numerical Methods for Scientists and Engineers", McGraw-Hill Book Company, Inc, New York, 1962.

DISTRIBUTION LIST — AFFTC-TDR-63-9

110 copies	—	Air Force Flight Test Center 6593d Test Group (Development) Edwards AFB, California
10 copies	—	Armed Services Technical Information Agency Arlington Hall Station Arlington 12, Virginia

Research & Technology Division, Edwards AF Base, Calif. Rpt No. RTD-TDR-63-9. EVALUATION AND MODIFICATION OF EXISTING PROTOTYPE DYNAMIC CALIBRATION SYSTEMS FOR PRESSURE-MEASURING TRANSDUCERS (U). Final Report, Mar 63, 70 p, incl illus, tables, 8 Refs. Unclassified Report Results are presented of an investigation of pressure transducer calibration facilities at EAFB and recommendations are made to improve this function.	1 Instrumentation I Project 3850 Task 38506 II Contract No AF 04(611)-8199 III Houston Engineering Research Corporation IV J L Schweppe J L Williams A H McMorris W R Busby V In ASTIA collection	Research & Technology Division, Edwards AF Base, Calif. Rpt No. RTD-TDR-63-9. EVALUATION AND MODIFICATION OF EXISTING PROTOTYPE DYNAMIC CALIBRATION SYSTEMS FOR PRESSURE-MEASURING TRANSDUCERS (U). Final Report, March 63, 70 p, incl illus, tables, 8 Refs. Unclassified Report Results are presented of an investigation of pressure transducer calibration facilities at EAFB and recommendations are made to improve this function.	1 Instrumentation I Project 3850 Task 38506 II Contract No AF 04(611)-8199 III Houston Engineering Research Corporation IV J L Schweppe J L Williams A H McMorris W R Busby V In ASTIA collection
Research & Technology Division, Edwards AF Base, Calif. Rpt No RTD-TDR-63-9. EVALUATION AND MODIFICATION OF EXISTING PROTOTYPE DYNAMIC CALIBRATION SYSTEMS FOR PRESSURE-MEASURING TRANSDUCERS (U). Final Report, March 63, 70 p, incl illus, tables, 8 Refs. Unclassified Report Results are presented of an investigation of pressure transducer calibration facilities at EAFB and recommendations are made to improve this function.	1 Instrumentation I Project 3850 Task 38506 II Contract No AF 04(611)-8199 III Houston Engineering Research Corporation IV J L Schweppe J L Williams A H McMorris W R Busby V In ASTIA collection	Research & Technology Division, Edwards AF Base, Calif. Rpt. No. RTD-TDR-63-9. EVALUATION AND MODIFICATION OF EXISTING PROTOTYPE DYNAMIC CALIBRATION SYSTEMS FOR PRESSURE-MEASURING TRANSDUCERS (U). Final Report, March 63, 70 p, incl illus, tables 8 Refs. Unclassified Report Results are presented of an investigation of pressure transducer calibration facilities at EAFB and recommendations are made to improve this function.	1 Instrumentation I Project 3850 Task 38506 II Contract No AF 04(611)-8199 III Houston Engineering Research Corporation IV J L Schweppe J L Williams A H McMorris W R Busby V In ASTIA collection